Beldar and Patil
Journal of Engineering and Applied Science (2024) 71:133
https://doi.org/10.1186/s44147-024-00468-w

Journal of Engineering and Applied Science

RESEARCH Open Access

A comparative study on engine vibration reduction in ATV quad bikes through dampers with diverse materials and shapes

Pankaj Beldar[1*] and Nivrutti Patil[1]

*Correspondence:
prbeldar@kkwagh.edu.in

[1] K. K. Wagh Institute of Engineering Education and Research, Nashik, India

Abstract

This study addresses the vital role of engine dampers in reducing vibrations and enhancing ride comfort in quad bikes. Utilizing ANSYS modal analysis and CATIA V5 design, the research aims to optimize damper design by assessing natural frequencies and potential resonance in the cage structure and engine. Through extensive analysis, the study evaluates vibrations transmitted from the engine to the chassis, crucial for understanding and improving overall vehicle performance. Neoprene rubber emerges as the optimal material for vibration dampers, offering superior density, elasticity, stiffness, and damping coefficient. Comparative analysis reveals that Design 3 of the dampers significantly outperforms Design 2 and Design 1, showcasing a remarkable 62% reduction in vibration. However, the study underscores the influence of various factors, such as application specificity and vibration characteristics, on damper effectiveness. Thus, while Design 3 may excel under certain conditions, careful consideration of diverse a variable is essential for optimal damper selection and performance across different engine types and operational contexts.

Keywords: Damper design, Structural optimization, Modal analysis, NVH, CATIA, Vibration, FFT analyzer

Introduction

Engine vibrations in all-terrain vehicles (ATVs) pose challenges to both vehicle performance and rider comfort [1]. As ATV usage expands across various terrains and applications, addressing these vibrations become paramount to enhance ride quality, minimize component wear, and ensure rider safety [2]. One crucial component in mitigating engine vibrations is the damper, designed to absorb and dissipate vibrational energy [3]. This paper presents a case study focused on reducing engine vibrations in an ATV quad bike through the implementation of different materials and shapes for the damper [4]. The significance of this study lies in its potential to enhance the overall performance and longevity of ATV quad bikes, while simultaneously improving rider comfort [5]. By exploring various damper materials and shapes, this research seeks to identify optimal configurations that effectively attenuate engine vibrations across a range of operating conditions [6]. The study employs a multidisciplinary approach, drawing on principles

from mechanical engineering, materials science, and vehicle dynamics [7]. Experimental testing, analytical modelling, and computational simulations are utilized to assess the performance of different damper configurations [8]. Through systematic evaluation, this research aims to provide valuable insights into the effectiveness of various damping solutions for ATV quad bikes. Fig. 1 shows the design process used in this paper.

Material selection

The first step in the design process is the selection of appropriate materials for the damper. Various factors such as damping capacity, durability, weight, and cost need to be considered [9]. Common materials for dampers include rubber compounds, viscoelastic polymers, and metal alloys. This study evaluates the mechanical properties and damping characteristics of different materials to determine their suitability for ATV damper applications [10].

Damper design

Once suitable materials are identified, the next step involves designing the damper geometry and configuration. Factors such as shape, size, and mounting arrangement are optimized to maximize damping efficiency while minimizing weight and space requirements [11]. Computer-aided design (CAD) software is used to model and simulate different damper designs, allowing for virtual testing and optimization before physical prototypes are fabricated [10].

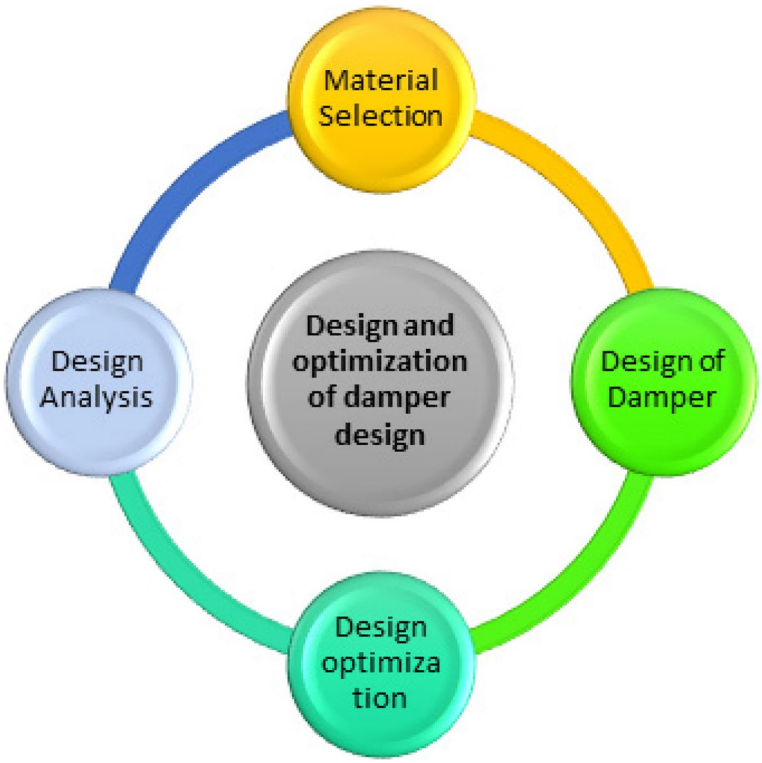

Fig. 1 Design process

Design optimization

The design optimization process aims to refine the damper configuration to achieve the best possible performance characteristics [7]. Iterative simulations and analyses are conducted to identify optimal design parameters such as material properties, geometry, and damping mechanisms. Advanced optimization algorithms and techniques, such as finite element analysis (FEA) and computational fluid dynamics (CFD), are employed to fine-tune the damper design and improve its effectiveness in reducing engine vibrations [1].

Analysis

Once the optimized damper design is obtained, comprehensive analysis is performed to assess its performance under various operating conditions. Analytical models are developed to predict damping performance, resonance frequencies, and stress distributions within the damper assembly. These analyses provide valuable insights into the behavior of the damper and help validate the design against performance requirements and specifications [3].

Experimental testing

Finally, experimental testing is conducted to validate the performance of the optimized damper design in real-world conditions. Physical prototypes are fabricated using the selected materials and manufacturing processes, and laboratory or field tests are conducted to measure damping efficiency, vibration reduction, and overall system response. The experimental results are compared with simulation data to verify the accuracy and effectiveness of the optimized damper design [12].

By integrating material selection, damper design, optimization, analysis, and experimental testing, this comprehensive approach provides a systematic framework for developing high-performance damping solutions for ATV quad bikes. The findings of this study contribute to advancements in ATV engineering and offer valuable insights for improving vehicle performance and rider comfort in off-road environments [13].

Review of related research

Maddaloni et al. [14] had looked at the fact that passive or active techniques can be used to dampen a building. In order to passively dissipate energy, passive methods rely on specific materials' innate capacity to absorb vibrational energy. Active methods employ sensors and actuators to detect vibrations, activate to stop them in real time, and achieve vibration detection. Additionally, piezoelectric components can be used as sensors and actuators. This review is primarily centered on passive damping materials, which were chosen because of their relative affordability and simplicity of use. Metals, polymers, cements, and their composites are examined as vibration-damping materials. Due of their viscoelasticity, metals and polymers are the dominant materials. However, it is appealing to employ concrete as a structural material to offer some dampening. Additionally, damping efficacy mostly involves mixture utilization in cement, interface design in polymers, and microstructural design in metals.

Das et al. [5] concluded that it is far simpler to distinguish between the reciprocating and rotational inertial forces of the connecting rod using this method than it is to analyze the inertial forces of a single cylinder engine through testing using expensive

machinery. According to the modelling results, the primary balance shaft and new crankshaft assembly are made in such a way as to entirely eliminate both the primary reciprocating inertial force and unbalanced rotational inertial force. The average bearing loads become the lowest, and the engine's NVH performance is significantly enhanced because the balanced mechanism is attached to lessen the unbalanced inertial forces. The reciprocating and rotational masses are divided in accordance with the results of the bearing loads simulation. In order to reduce the engine's noise, vibration, and harshness, a new balanced mechanism is built, and the simulation results demonstrate that it is completely balanced in inertial force.

Lundqvist et al. [13] studied the damping coefficient of a single cylinder in terms of the crank angle position that is theoretically determined in this review through a study of relative quasi-static experiment. The technique is based on the formulation of the vibratory energy balance, and it makes use of the measured torsional response of the setup's limiting points. Additionally, a matching motor experiment can be utilized to measure the average damping that is seen when the engine is running. This average damping fits the numerically calculated time-average damping data reasonably well. The linear analysis of reciprocating engine systems with one or more cylinders is carried out using the resulting damping coefficient. Another intriguing outcome of this investigation demonstrates the dampening effect in the crank-connecting rod. The net damping level seen in the reciprocating sections must be less than the dominance of the interacting areas. We can determine the damping coefficient of a vertical single cylinder internal combustion engine even though the proposed method is presented on a reciprocating single-cylinder engine setup because its essential principles apply to various damping elements in the powertrain system.

Zhou and colleagues [15] conducted an experimental study focusing on the mechanical properties of hybrid lead viscoelastic dampers. Their research aimed to enhance the understanding of hybrid lead viscoelastic dampers and explore their potential applications in structural engineering. By investigating the mechanical behavior of these dampers, they provided valuable insights into their effectiveness in mitigating vibrations and enhancing the resilience of structures to dynamic loads.

Modhej et al. [16] investigated pre-tensioned shape memory alloy (SMA) cable tests and their application in a novel self-centering viscoelastic damper. Their study delved into innovative damping technologies with potential applications in seismic-resistant design. By exploring the performance of pre-tensioned SMA cables in self-centering dampers, they contributed to the development of advanced seismic mitigation strategies, aiming to improve the resilience of structures to earthquakes and other dynamic events. Narchasanah [17] and collaborators explored the properties and design of engine mounting rubber automotive as dampers for building retrofitting. Their research emphasized the significance of utilizing automotive rubber dampers in retrofitting structures to enhance seismic performance. By investigating the mechanical properties and design considerations of these dampers, they provided valuable guidance for engineers and practitioners involved in retrofitting existing buildings for improved resilience to seismic events. In this study [18], Widya Prasetya and team proposed a design for rubber dampers in electric inspection trucks, aiming to improve the damping performance of inspection vehicles in the field of transportation engineering. Their research addressed

the challenges associated with vibration control in inspection vehicles, offering innovative solutions to enhance vehicle stability, comfort, and reliability during operation. Qian et al. [19] conducted shake table investigations on structures isolated by recycled rubber devices and magneto rheological dampers. Their research focused on seismic isolation techniques using innovative damping technologies. By evaluating the performance of structures isolated by recycled rubber devices and magneto rheological dampers under simulated seismic loads, they provided valuable insights into the effectiveness of these damping systems in enhancing the seismic resilience of structures. Rajkumar et al. [20] conducted experimental studies and mathematical modeling of viscoelastic dampers with wider temperature ranges based on blended rubber matrix. Their research aimed to develop viscoelastic damping materials with improved performance under varying environmental conditions. By investigating the mechanical properties and temperature sensitivity of these dampers, they contributed to the advancement of damping technologies for applications in diverse engineering fields. In this study [21], Modhej and Zahrai performed experimental studies on high axial damping rubber (HADR) in new viscoelastic dampers. Their research focused on evaluating the performance of HADR in damping applications, aiming to improve the damping capacity of viscoelastic dampers for structural and mechanical systems. By investigating the mechanical properties and damping characteristics of HADR, they provided valuable data for the development of advanced damping materials and technologies. Sunkato et al. [22] evaluated the vibration characteristics and handle vibration damping of diesel-fueled 15-HP single-axle tractors. Their research addressed the challenges associated with vibration control in agricultural machinery, aiming to improve operator comfort and reduce fatigue during tractor operation. By analyzing the vibration characteristics and damping performance of tractors, they provided insights into the effectiveness of damping solutions for enhancing the ergonomic design of agricultural equipment. Becker et al. [2] conducted experimental studies on high-damping viscoelastic rubber coupling beam dampers. Their research focused on exploring the behavior and performance of rubber coupling beam dampers in structural engineering applications. By evaluating the damping capacity and energy dissipation characteristics of these dampers, they provided valuable insights into their effectiveness in mitigating vibrations and enhancing the seismic resilience of structures. Toma et al. [23] estimated the damping ratio of silicone rubber using the half power bandwidth method. Their research aimed to develop a methodology for assessing the damping properties of silicone rubber materials, which are commonly used in various engineering applications. By analyzing the damping characteristics of silicone rubber, they provided valuable data for optimizing the design and performance of damping systems in engineering practice. Clay et al. [4] investigated high-damping rubber dampers for taut cable vibration reduction. Their research focused on developing innovative solutions for mitigating vibrations in cable structures, aiming to improve the stability and performance of cable-supported systems. By evaluating the damping characteristics and vibration reduction capabilities of high-damping rubber dampers, they provided insights into their effectiveness in enhancing the dynamic behavior of cable structures. These studies collectively contribute to the advancement of damping technologies and their applications across various engineering disciplines. By investigating the mechanical properties,

Methods

The methodology as shown in Fig. 2 employed in this research paper encompasses a structured approach aimed at comprehensively addressing the challenges associated with optimizing engine dampers for enhanced NVH (noise, vibration, and harshness) performance in ATV quad bikes [11]. Initially, the study delves into understanding the detrimental effects of vibration resonances on system integrity and lifespan, followed by a meticulous evaluation of the dynamic forces exerted by engine excitation on the mounting system. Subsequently, a proposed design methodology is outlined, involving the modeling of dampers while adhering to specified design limitations and scrutinizing various materials to ascertain optimal dampening characteristics. Through iterative testing, materials are systematically evaluated to identify the most effective solution [10]. The analysis phase validates the proposed design's stress and deflection, ensuring compliance with safety and performance standards. Leveraging ALTAIR Inspire software, structural optimization techniques are applied to refine the damper design for improved

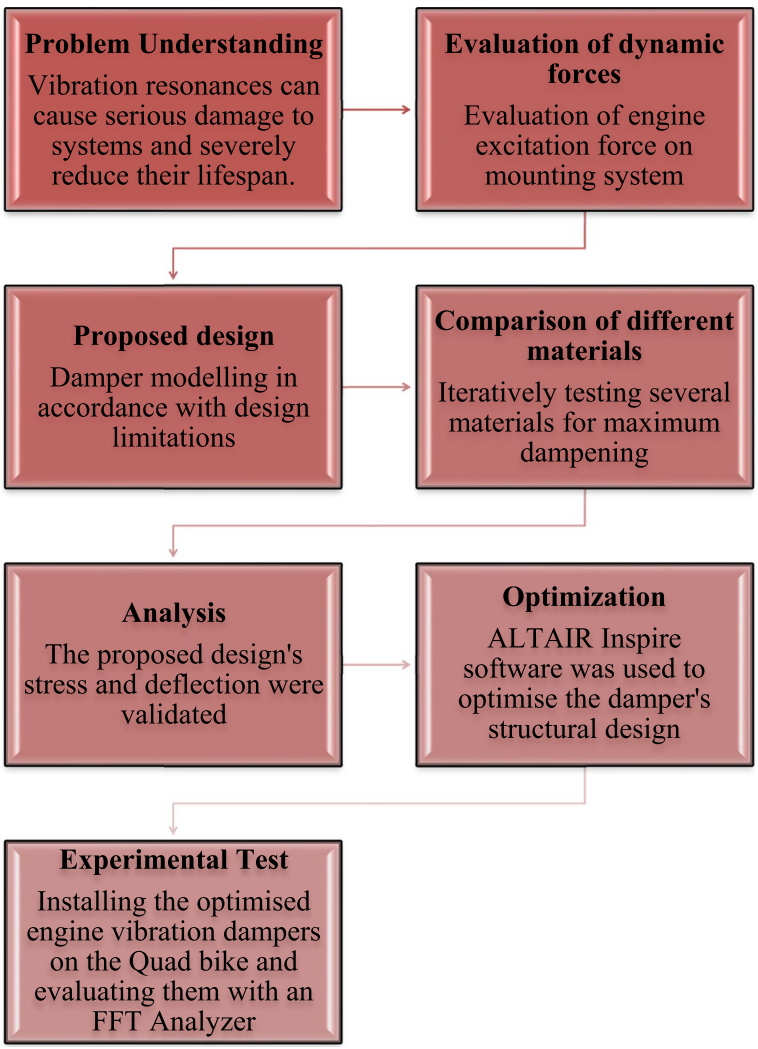

Fig. 2 Methodology

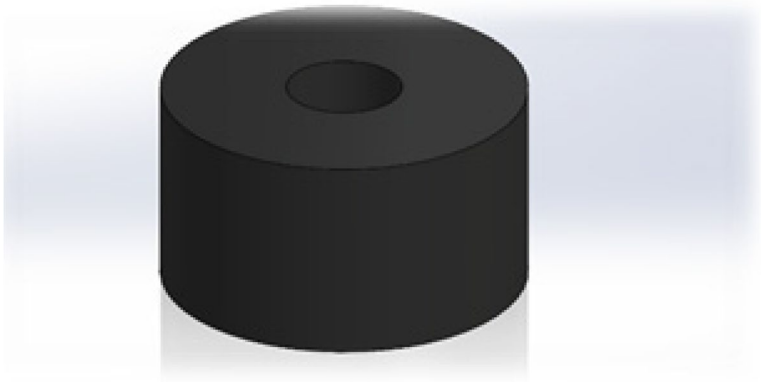

Fig. 3 Existing design 1

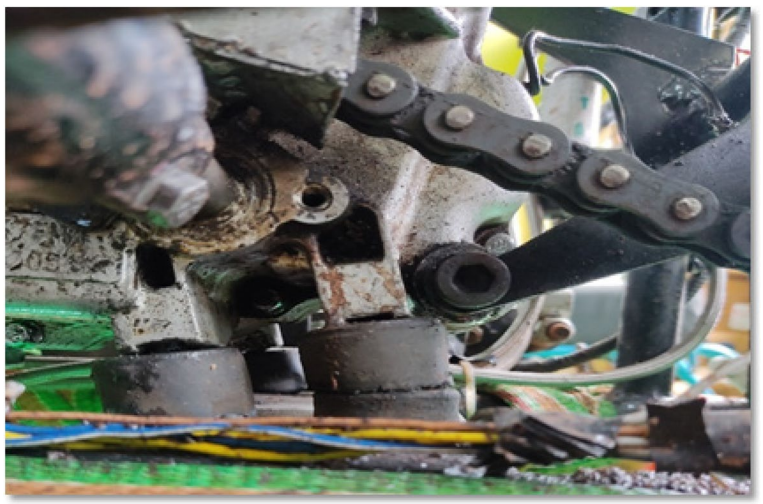

Fig. 4 Position of damper

efficiency. Experimental validation entails the installation of optimized dampers on quad bikes, with performance evaluation conducted using an FFT Analyzer under real-world conditions. This iterative process aims to iteratively refine the damper design, ensuring it effectively mitigates engine vibrations, thereby enhancing the overall ride quality and comfort of ATV quad bikes [11].

Proposed design

Figure 3 shows the existing design of damper used in ATV, and Fig. 4 shows the position of damper in ATV.

Concept design

Figures 5 and 6 shows the concept designs 2 and 3 of damper.

The shapes of concept designs 2 and 3 are selected as per geometry of engine base. It is proposed shape that can be helpful for proper support of the engine. The original shape of damper is circular which has problem of proper support; hence, non-circular shapes are selected for further analysis and support.

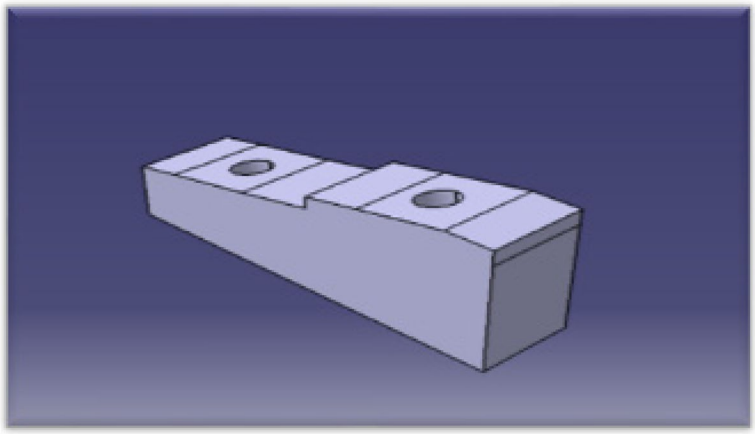

Fig. 5 Concept design 2

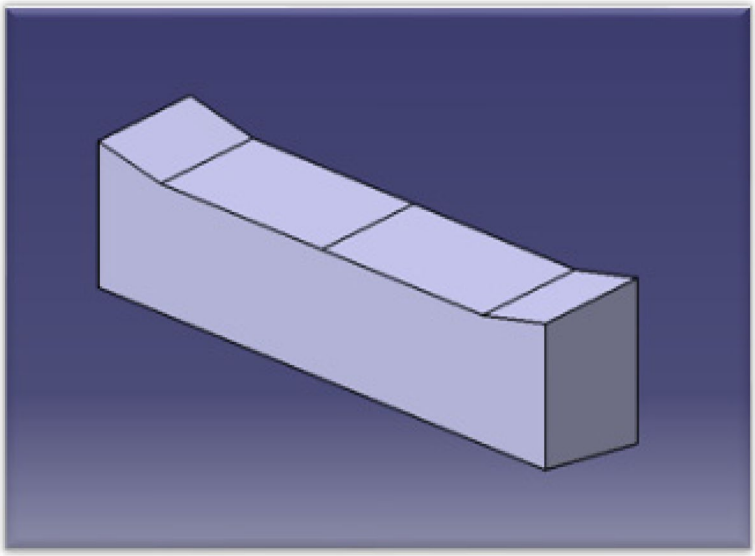

Fig. 6 Concept design 3

Material and properties

Table 1 provides the material properties of different materials consider for design the damper.

Dynamic forces calculation [27]

Piston ring = 0.254 kg

Connecting rod = 0.500 kg

Mass of Reciprocating mass = $\frac{(0.254+0.500)*1}{3}$

M = 0.2513 kg

where,

r= 0.0325 m

Table 1 Material properties

Properties	Materials [24–26]		
	Nitrile	Neoprene	Polyurethane
Density (g/cm^3)	0.97	1.22	1.06
Young modulus (MPa)	4	2.5	6
Bulk modulus (MPa)	666.6	416	999.11
Shear modulus (MPa)	1.3	0.833	2
Coefficient of thermal expansion (10-6)	150	139	250
Damping ratio	0.05	0.05	0.05

$W = 733$ RPS

$\theta = 0^\circ$

$C = 1/3 = 0.33$

Now,

$$F = mw^2r * \left[\sqrt{(1-c)^2\ Cos2\theta + c^2\ Sin^2\theta}\right] \quad (1)$$

$F = mrw^2 * (1\text{-}c)$

Put all values in Eq. (1):

$F = 0.2513 * 0.0325 * (733)^2[1 - (2/3)]$

$F = 1462.74$ N

That is, the forces considered on it are as follows:

(i) Inertial forces from engine = 1462.74 N

(ii) The weight of engine = m * g

Where,

$m = 34$ kg

$m = 34 * 9.81$

$m = 333.54$ N

Total force = inertial Force + Weight of engine

$= 1462.74 + 333.54$

$= 1796.28$ N

In the dynamic force calculation for a damper, several factors come into play to determine the forces acting on it. Firstly, the mass of the reciprocating components involved, such as the piston ring and connecting rod, needs to be determined. These components contribute to the reciprocating mass, which influences the inertial forces during operation.

Once the reciprocating mass is established, parameters like the radius of rotation (r) and the angular velocity (ω) of the engine are considered. These parameters, along with the cosine and sine of the angle of rotation (θ), are used in the dynamic force equation to calculate the force acting on the damper.

The dynamic force equation incorporates the reciprocating mass, angular velocity, radius of rotation, and a damping factor (c). This damping factor represents the ratio of the mass of the reciprocating components to the total mass of the system. It

is crucial in determining the effectiveness of the damper in reducing vibration and oscillations.

By substituting the given values into the dynamic force equation, the inertial forces acting on the damper can be calculated. These forces represent the resistance encountered by the damper due to the reciprocating motion of the engine components.

In addition to inertial forces, the weight of the engine itself needs to be considered another force acting on the damper. This weight is calculated based on the mass of the engine and the acceleration due to gravity.

Finally, the total force acting on the damper is determined by adding the inertial forces and the weight of the engine. This total force provides insight into the magnitude of the dynamic loads that the damper must withstand during engine operation.

Modal analysis of concept design 2

Modal analysis is pivotal in a study on reducing engine vibrations in ATV quad bikes with different dampers. It helps understand the quad bike's dynamic behavior, evaluate dampers' effectiveness, and optimize their design. By analyzing natural frequencies, mode shapes, and damping ratios, engineers can identify the most efficient damping solutions. This ensures robust strategies to mitigate engine vibrations and enhance quad bike performance.

The modal analysis results provide crucial insights into the vibrational characteristics of the Neoprene damper, which is essential for its effective design and performance optimization. Each mode corresponds to a specific natural frequency at which the damper system tends to vibrate, offering valuable information for understanding its dynamic behavior and potential resonance issues [28].

Modal analysis is indispensable for damper design as it enables engineers to identify critical modes of vibration and assess their impact on overall system performance. By understanding the natural frequencies and mode shapes, designers can tailor the damper's characteristics to effectively mitigate vibrations and enhance system stability and durability [29].

Mathematically, the natural frequency (fn) of a vibrating system can be expressed using the formula [28, 30]:

$$fn = \frac{1}{2\pi}\sqrt{\frac{k}{m}}$$

Where,

fn is the natural frequency

k is the stiffness of the damper

m is the mass of the damper

This expression illustrates the relationship between the stiffness and mass of the damper, indicating that higher stiffness or lower mass results in higher natural frequencies. By manipulating these parameters during the design phase, engineers can tailor the damper's characteristics to meet specific performance requirements and mitigate resonant vibrations effectively.

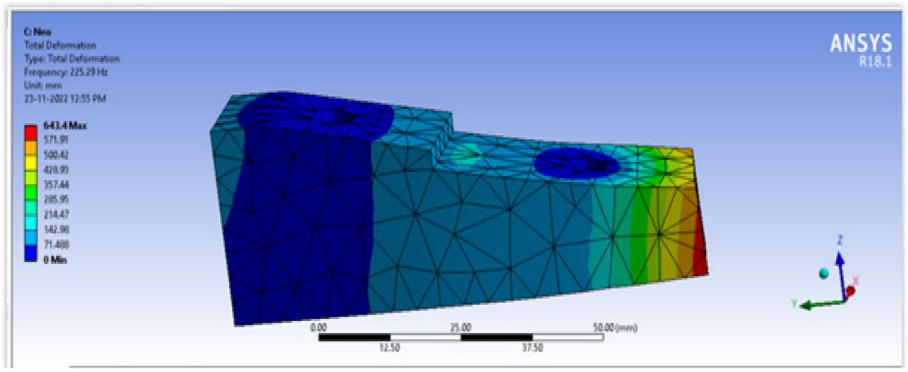

Fig. 7 Mode shape 1 for neoprene damper

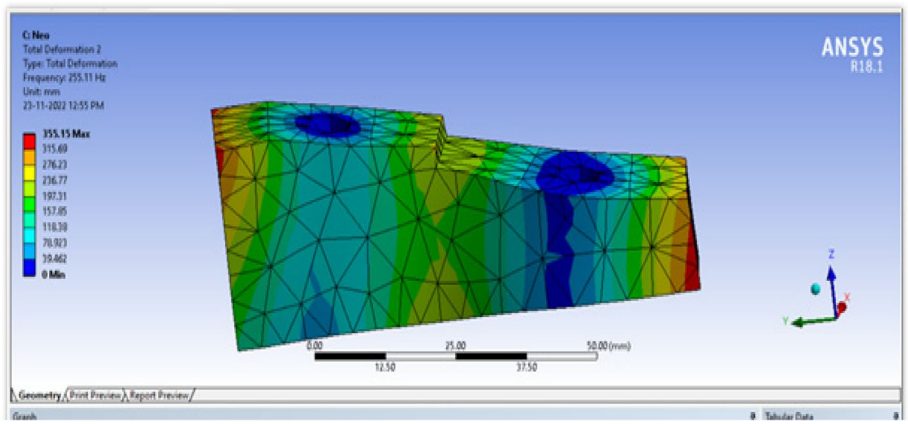

Fig. 8 Mode shape 2 for neoprene damper

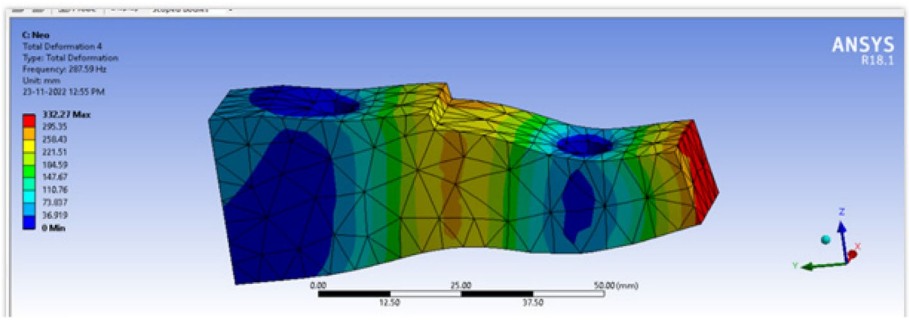

Fig. 9 Mode shape 3 for neoprene damper

Modal analysis of neoprene damper

Figures 7, 8, 9, 10, 11 and 12 show the corresponding mode shapes for neoprene damper of concept design 2.

The frequencies associated with each mode reveal the vibrational modes of the damper, with higher modes indicating higher frequencies of vibration. For instance, the first mode exhibits a frequency of 225.29 Hz, while subsequent modes progressively increase in frequency, with the sixth mode reaching 318.41 Hz. This progression

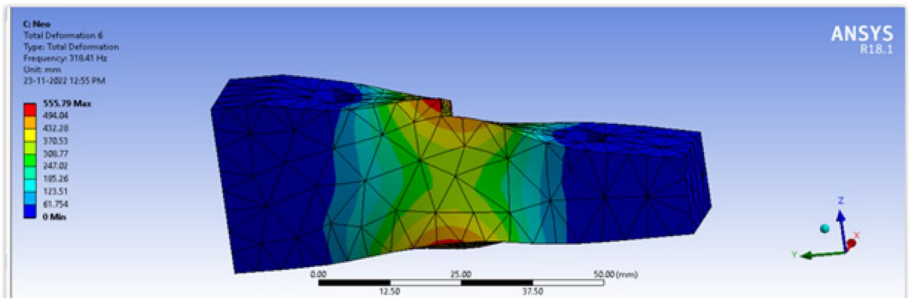

Fig. 10 Mode shape 4 for neoprene damper

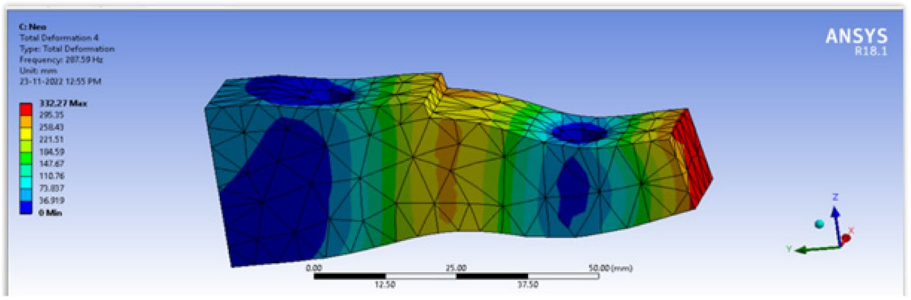

Fig. 11 Mode shape 5 for neoprene damper

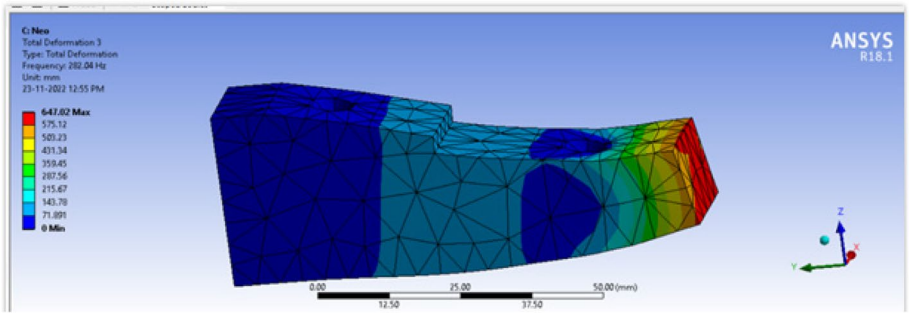

Fig. 12 Mode shape 6 for neoprene damper

highlights the diverse vibrational modes inherent in the damper system and underscores the importance of considering multiple modes in the design and analysis process.

Modal analysis of nitrile damper

Figures 13, 14, 15, 16, 17 and 18 show the corresponding mode shapes for nitrile damper of concept design 2.

Examining the results, we observe a progressive increase in frequency across different modes, with the first mode exhibiting a frequency of 320.89 Hz and the sixth mode reaching 453.53 Hz. This pattern indicates the diverse vibrational modes present in the nitrile rubber damper, highlighting the need for comprehensive modal analysis to identify critical modes and their potential impact on system behavior.

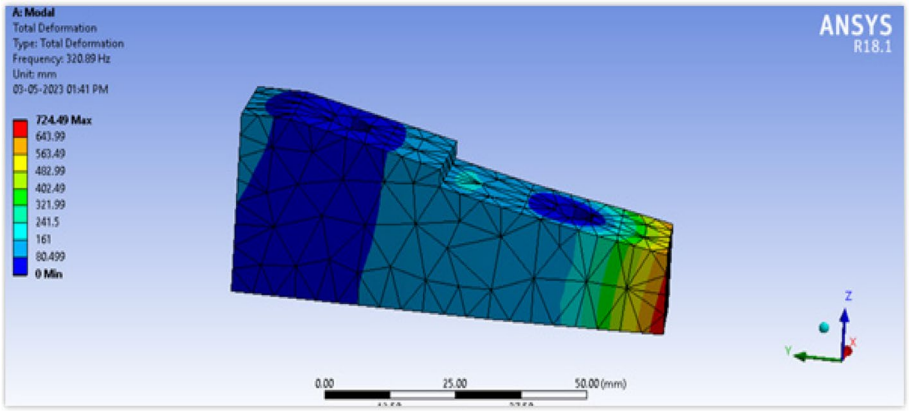

Fig. 13 Mode shape 1 for nitrile damper

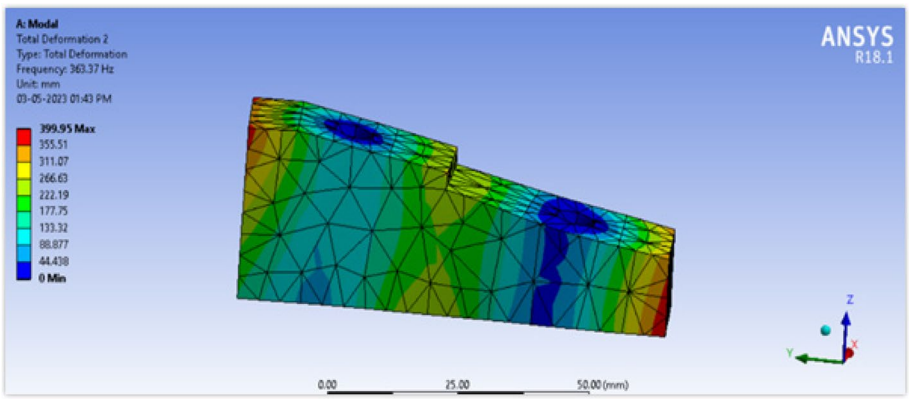

Fig. 14 Mode shape 2 for nitrile damper

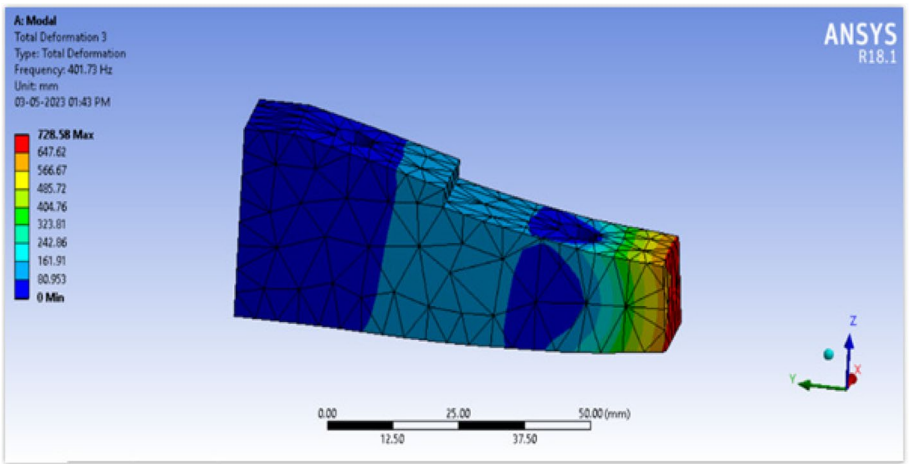

Fig. 15 Mode shape 3 for nitrile damper

Modal analysis of polyurethane damper

Figures 19, 20, 21, 22, 23 and 24 show the corresponding mode shapes for polyurethane damper of concept design 2.

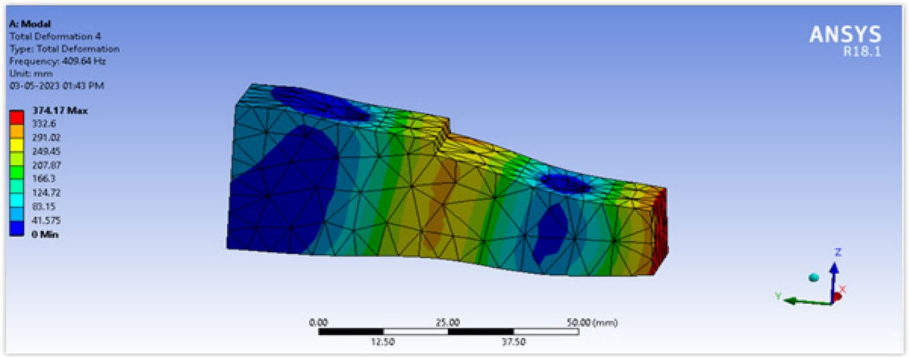

Fig. 16 Mode shape 4 for nitrile damper

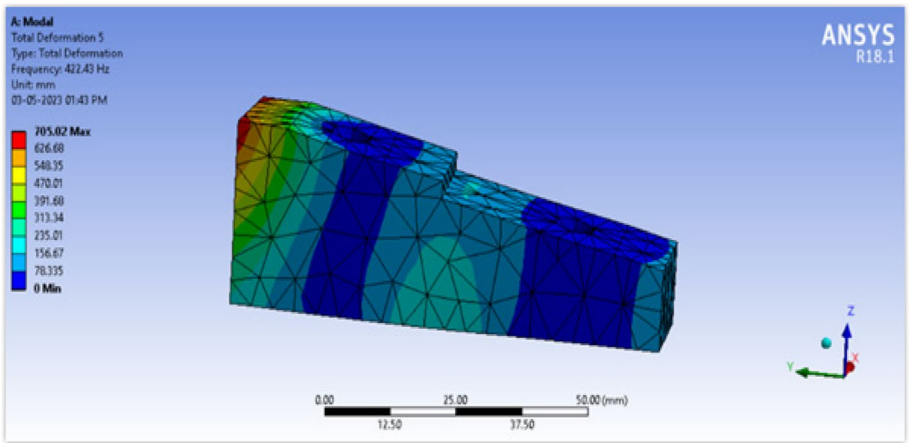

Fig. 17 Mode shape 5 for nitrile damper

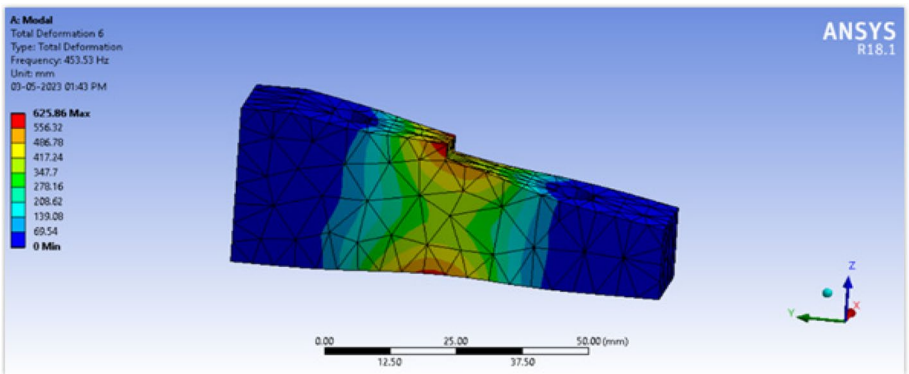

Fig. 18 Mode shape 6 for nitrile damper

Upon examination of the results, we observe a progressive increase in frequency across different modes. The first mode exhibits a frequency of 375.95 Hz, while the sixth mode reaches 531.35 Hz. This trend indicates the diverse vibrational modes

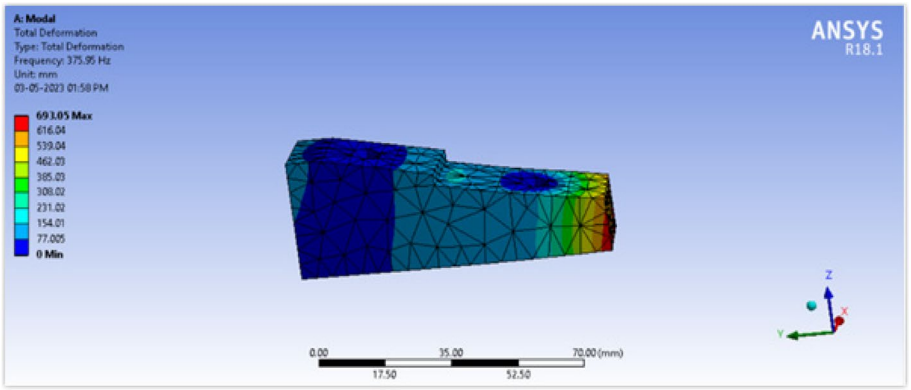

Fig. 19 Mode shape 1 for polyurethane damper

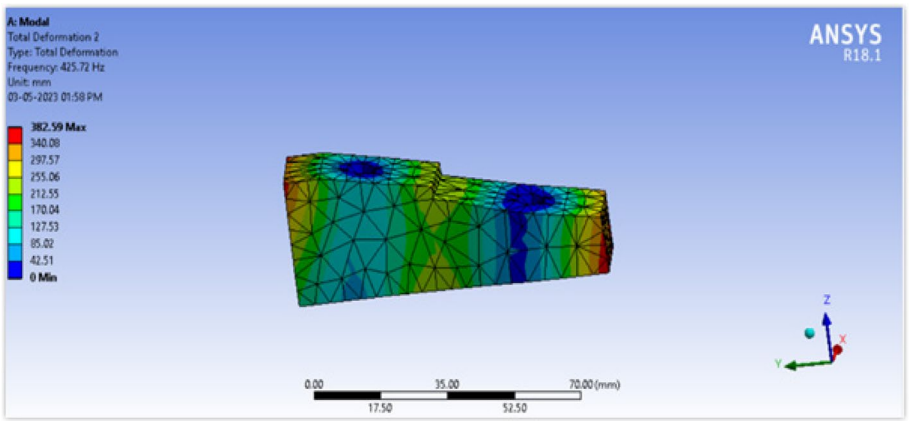

Fig. 20 Mode shape 2 for polyurethane damper

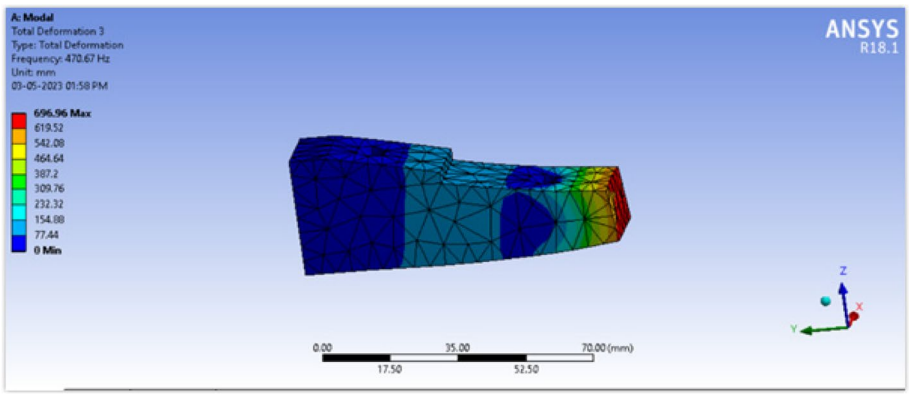

Fig. 21 Mode shape 3 for polyurethane damper

present in the polyurethane damper, underscoring the necessity of conducting comprehensive modal analysis to identify critical modes and their potential impact on system behavior.

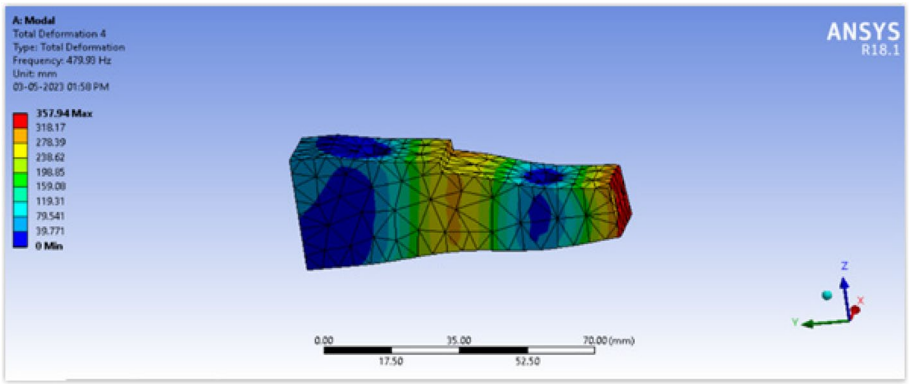

Fig. 22 Mode shape 4 for polyurethane damper

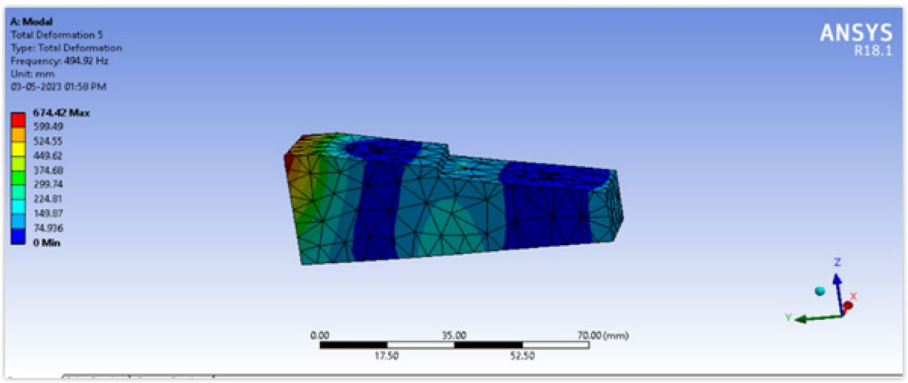

Fig. 23 Mode shape 5 for polyurethane damper

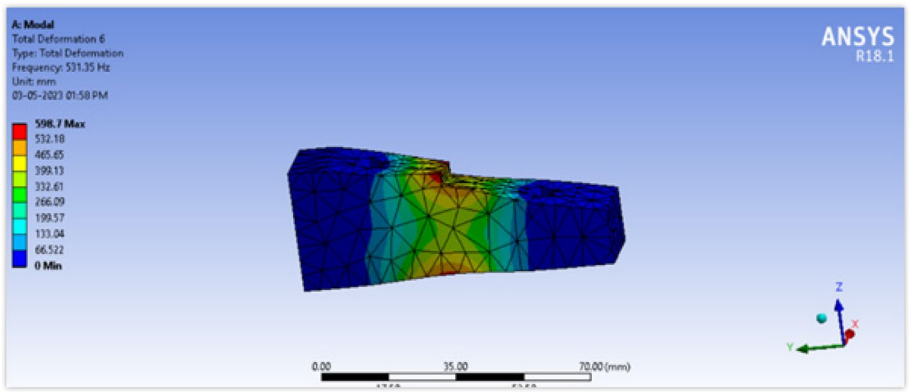

Fig. 24 Mode shape 6 for polyurethane damper

Table 2 shows the modal analysis of different types of damper of concept design 2.

The modal analysis results indicate that neoprene dampers exhibit lower natural frequencies compared to nitrile and polyurethane dampers. This suggests that neoprene may be better at attenuating lower frequency vibrations, suitable for ATV quad bikes. Nitrile and polyurethane dampers, with higher natural frequencies, may be

Table 2 Modal analysis of concept design 2

Modal analysis of neoprene damper		Modal analysis of nitrile damper		Modal analysis of polyurethane damper	
Mode	**Frequency (Hz)**	**Mode**	**Frequency (Hz)**	**Mode**	**Frequency (Hz)**
1	225.29	1	320.89	1	375.95
2	255.11	2	363.37	2	425.72
3	282.04	3	401.73	3	470.67
4	287.99	4	409.64	4	479.93
5	296.58	5	422.43	5	494
6	318.41	6	453.53	6	531.35

more effective in mitigating higher frequency vibrations, beneficial for off-road terrain or high-speed operation. Material selection is critical, with each offering unique vibrational properties. Further testing is necessary to confirm performance under real-world conditions.

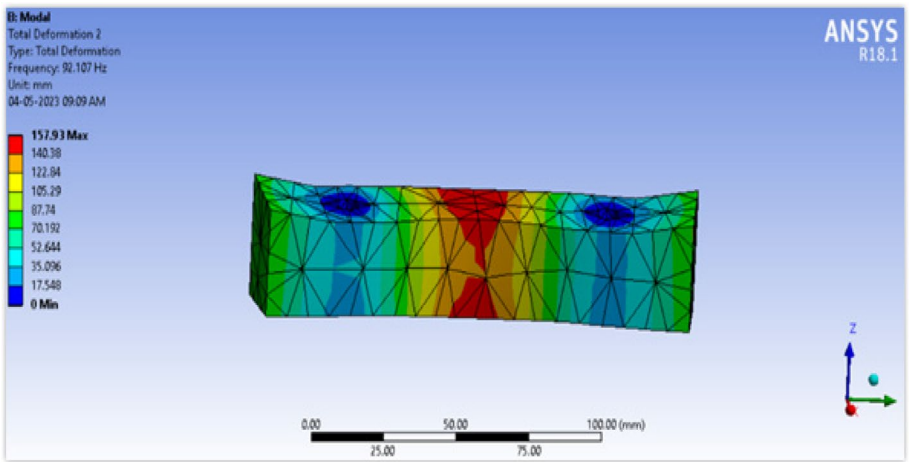

Fig. 25 Mode shape 1 for neoprene damper

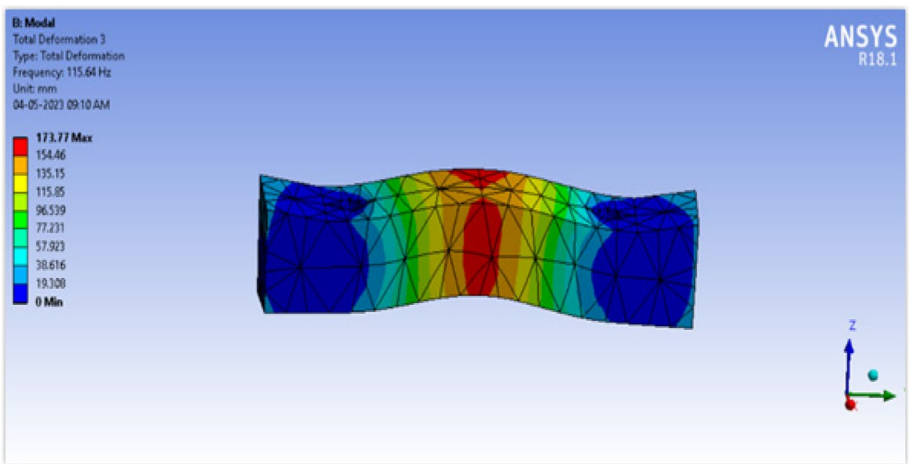

Fig. 26 Mode shape 2 for neoprene damper

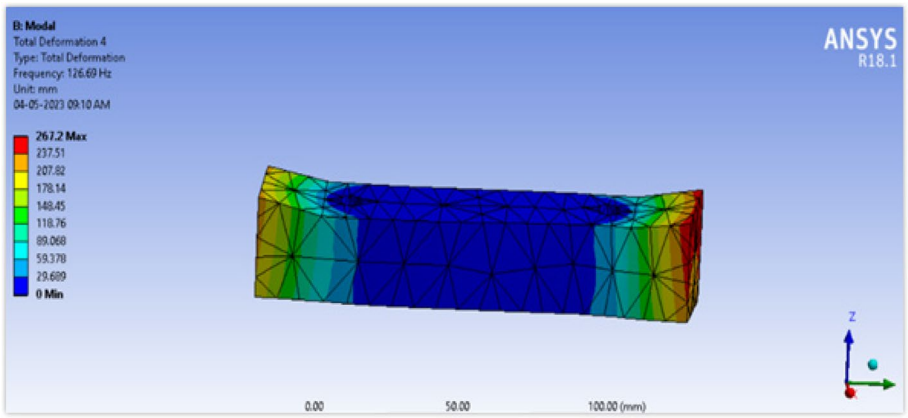

Fig. 27 Mode shape 3 for neoprene damper

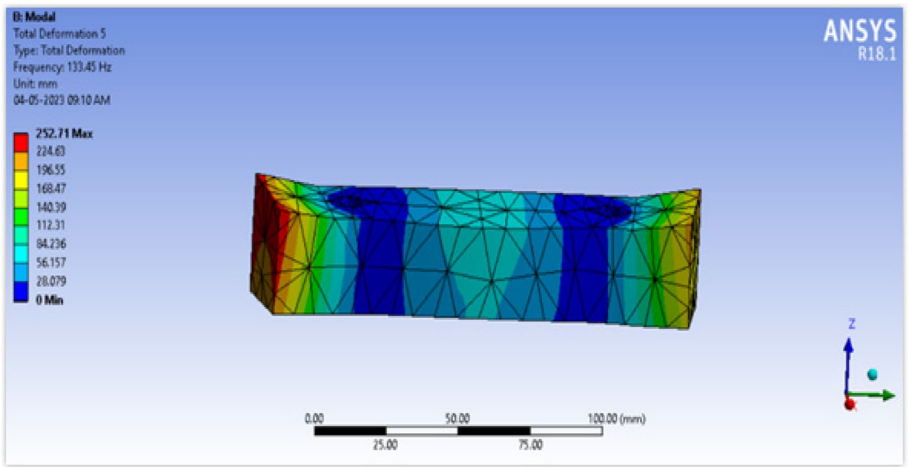

Fig. 28 Mode shape 4 for neoprene damper

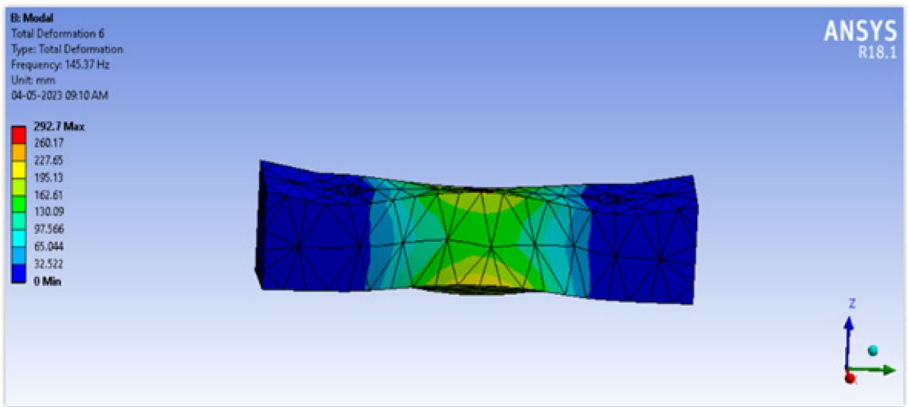

Fig. 29 Mode shape 5 for neoprene damper

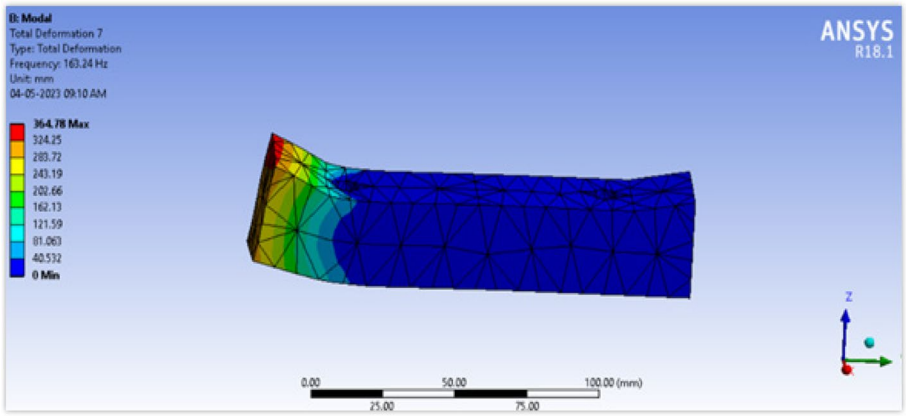

Fig. 30 Mode shape 6 for neoprene damper

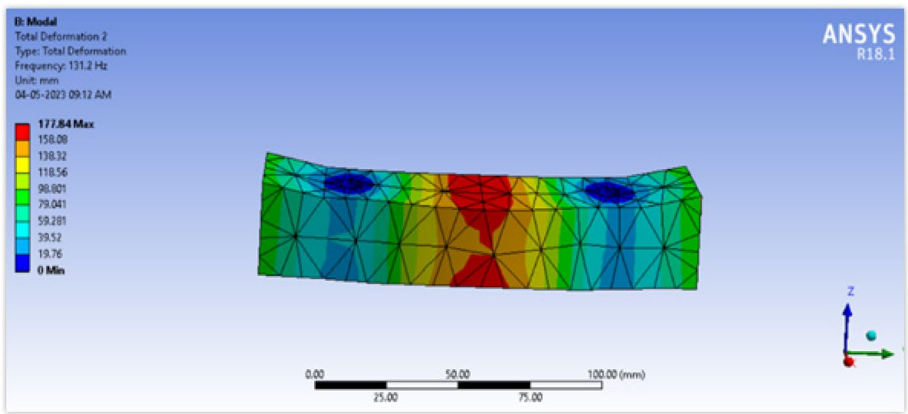

Fig. 31 Mode shape 1 for polyurethane damper

Modal analysis of concept design 3

Modal analysis of neoprene damper

Figures 25, 26, 27, 28, 29 and 30 show the corresponding mode shapes for neoprene damper of concept design 3.

Modal analysis of polyurethane damper

Figures 31, 32, 33, 34, 35 and 36 show the corresponding mode shapes for polyurethane damper of concept design 3.

Modal analysis of nitrile damper

Figures 37, 38, 39, 40, 41 and 42 shows the corresponding mode shapes for nitrile damper of concept design 3.

Table 3 shows the modal analysis of different types of damper of concept design 3.

The modal analysis results for neoprene, nitrile, and polyurethane dampers in concept design 2 reveal distinct vibrational characteristics. Neoprene dampers exhibit the lowest natural frequencies across all modes, indicating potential effectiveness in attenuating low-frequency vibrations. Nitrile and polyurethane dampers show higher natural

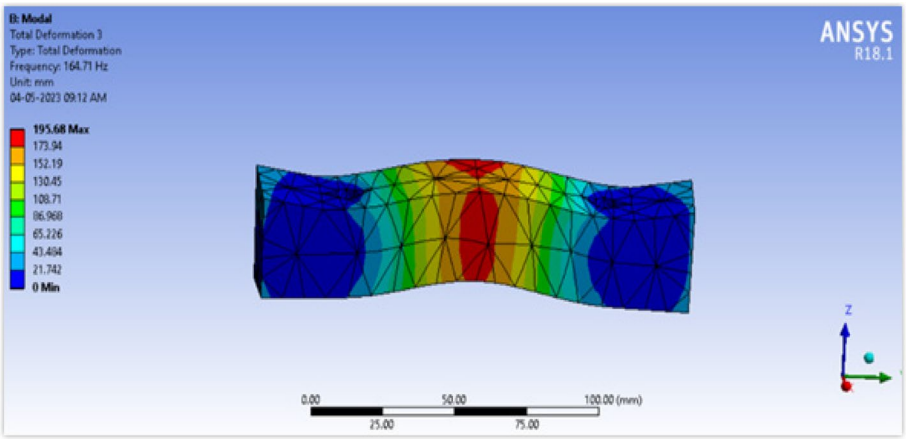

Fig. 32 Mode shape 2 for polyurethane damper

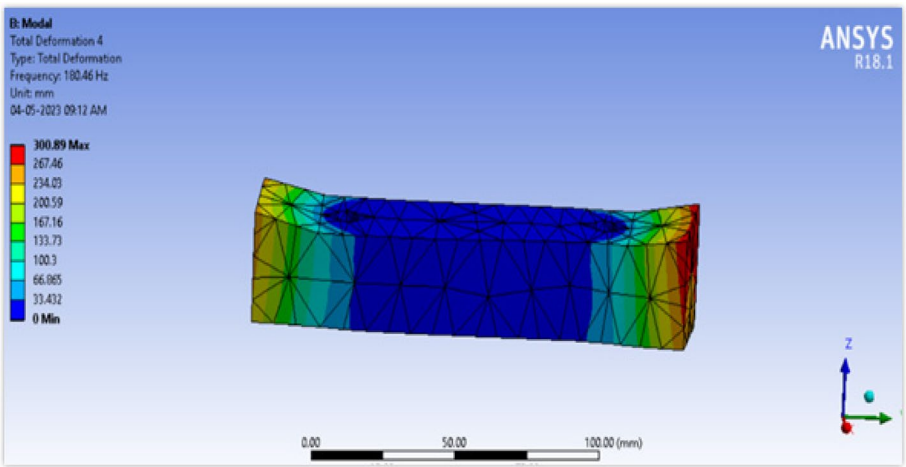

Fig. 33 Mode shape 3 for polyurethane damper

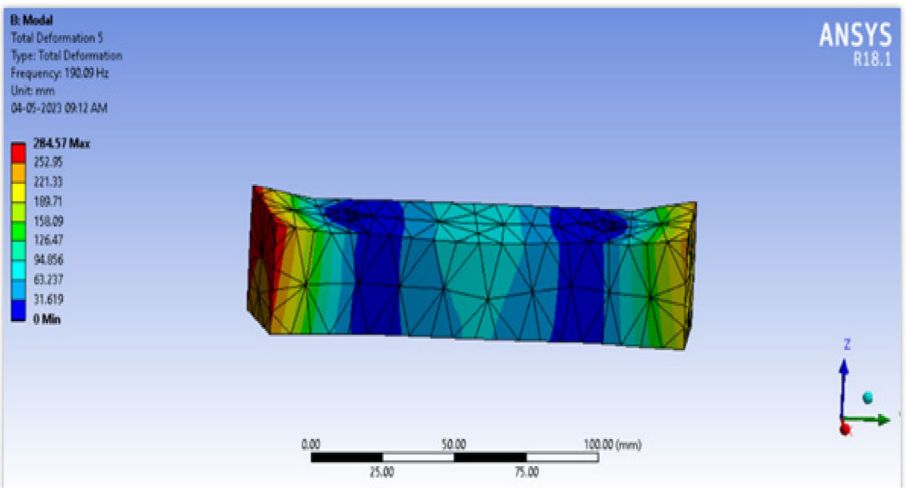

Fig. 34 Mode shape 4 for polyurethane damper

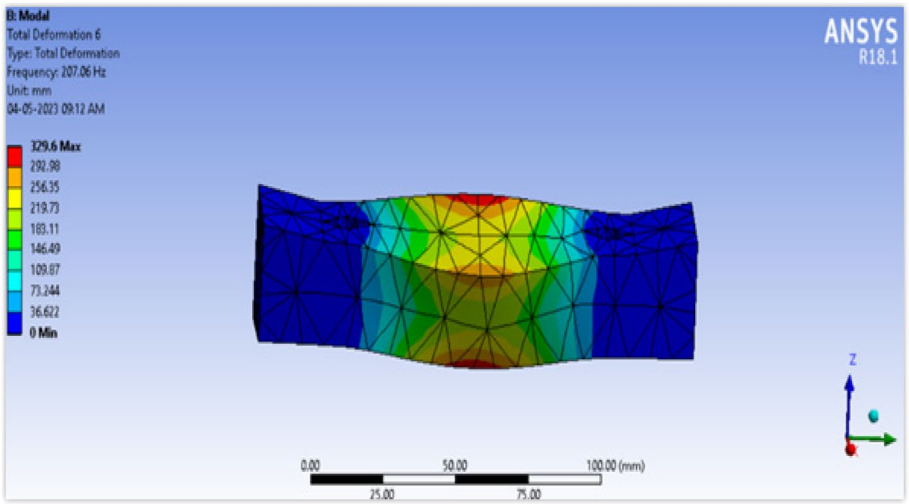

Fig. 35 Mode shape 5 for polyurethane damper

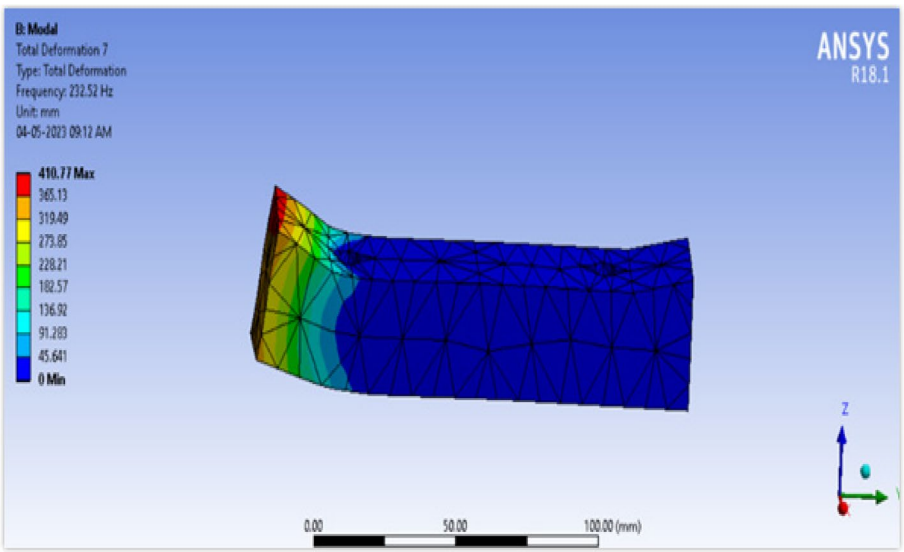

Fig. 36 Mode shape 6 for polyurethane damper

frequencies, suggesting suitability for mitigating higher frequency vibrations, beneficial for off-road terrain or high-speed operation. Material selection remains critical, with each offering unique vibrational properties. Further testing is necessary to validate performance in real-world conditions.

Experimental testing

Below, Figs. 43, 44 and 45 show the design 1 of different materials.

Below, Figs. 46, 47 and 48 show the design 2 of different materials.

Below, Figs. 49, 50 and 51 show the design 3 of different materials.

The utilization of the SKF Microlog Analyzer CMXA 75, coupled with the SKF Probe CMSS 2200, underscores a commitment to precise and efficient experimental

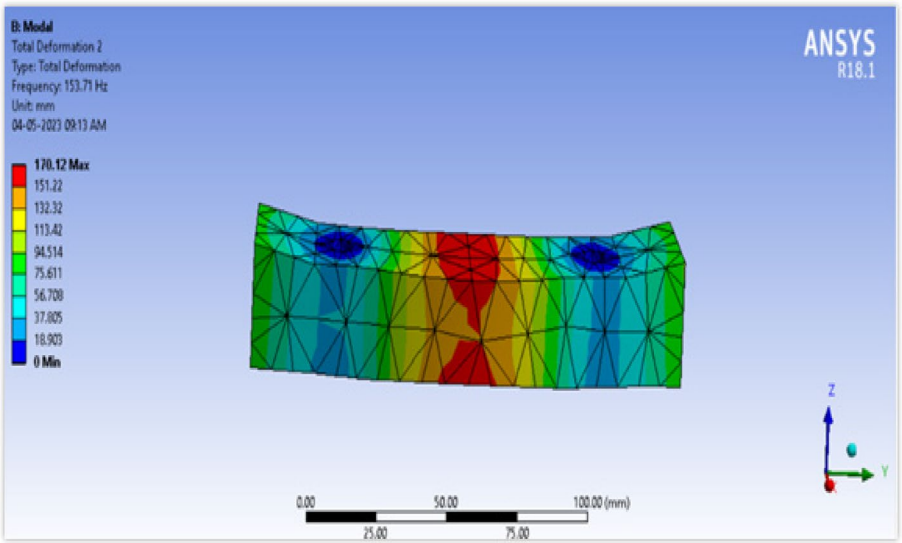

Fig. 37 Mode shape 1 for nitrile damper

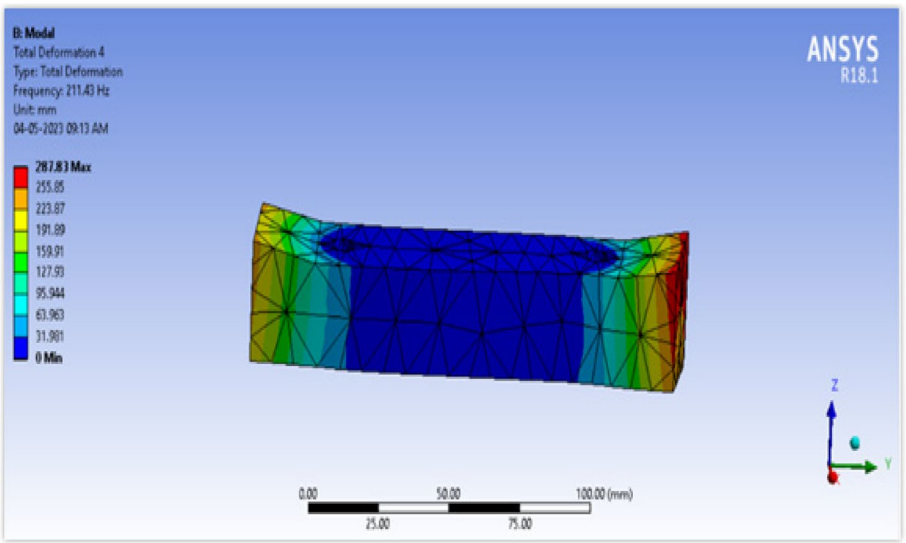

Fig. 38 Mode shape 3 for nitrile damper

testing in the realm of vibration analysis and condition monitoring. The analyzer boasts a Marvell 806 MHz PXA320 processor, ensuring exceptionally fast operation crucial for real-time data collection and analysis. Its rugged design, withstanding two-meter multiple drops and IP 65 rating, guarantees durability and reliability in diverse industrial environments.

The analyzer as shown in Fig. 52 offers a broad frequency range from DC to 80 kHz, allowing for comprehensive assessment of vibration signals across a wide spectrum. With an accuracy of +2.5% of the full-scale range and FFT resolution ranging from 100 to 25,600 lines, the analyzer provides precise and detailed insights into vibration characteristics and behavior.

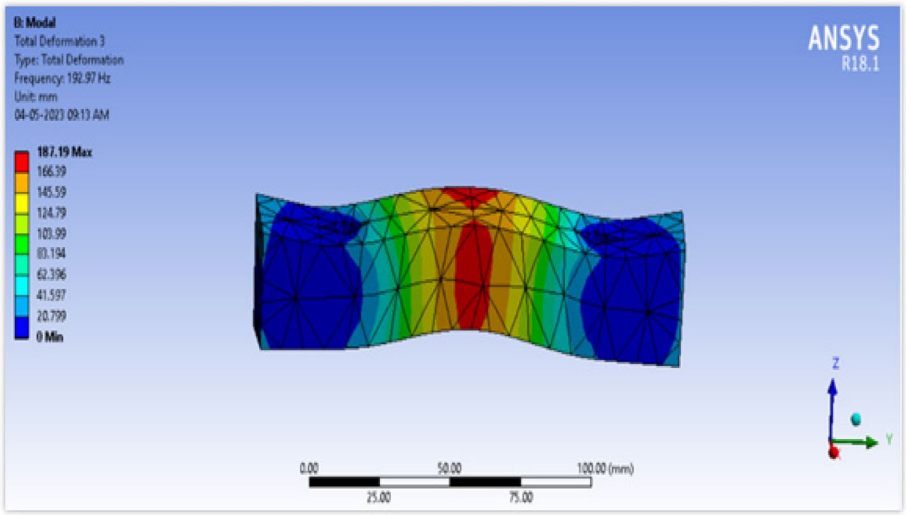

Fig. 39 Mode shape 2 for nitrile damper

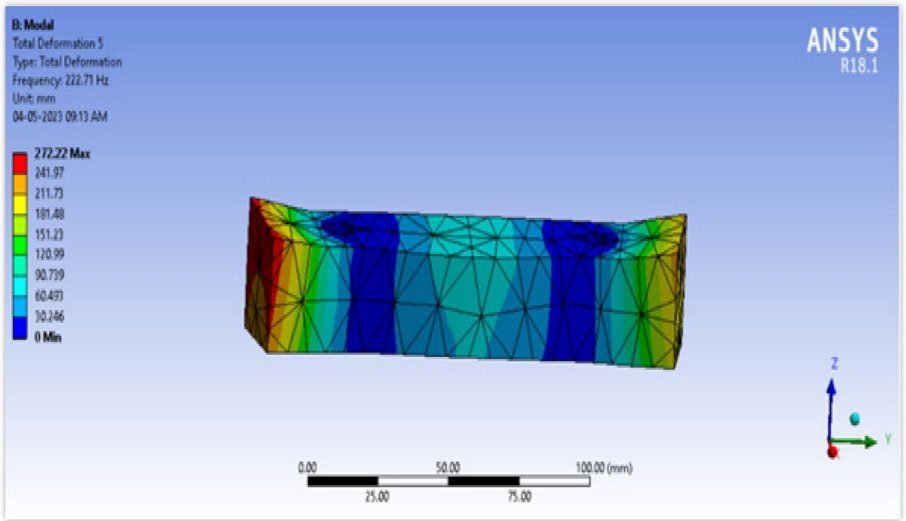

Fig. 40 Mode shape 4 for nitrile damper

Additionally, the provision of a tachometer power supply output at 5V enables seamless integration with various sensors and equipment for synchronized data collection. The analyzer's robust input over-voltage protection, accommodating AC250V peak and DC 250V, ensures the safety of the equipment and personnel during operation.

Complementing the analyzer, the SKF Probe CMSS 2200 shown in Fig. 53 offers a versatile solution for vibration measurement, featuring a general-purpose, low-profile design with a side exit. With a sensitivity of 100 mVg and precise sensitivity precision of ±10% at 25 °C, the probe delivers accurate and reliable measurements. Its measurement range of 80 g peak and broad frequency range from 1.0 to 10,000 Hz further enhances its suitability for various industrial applications.

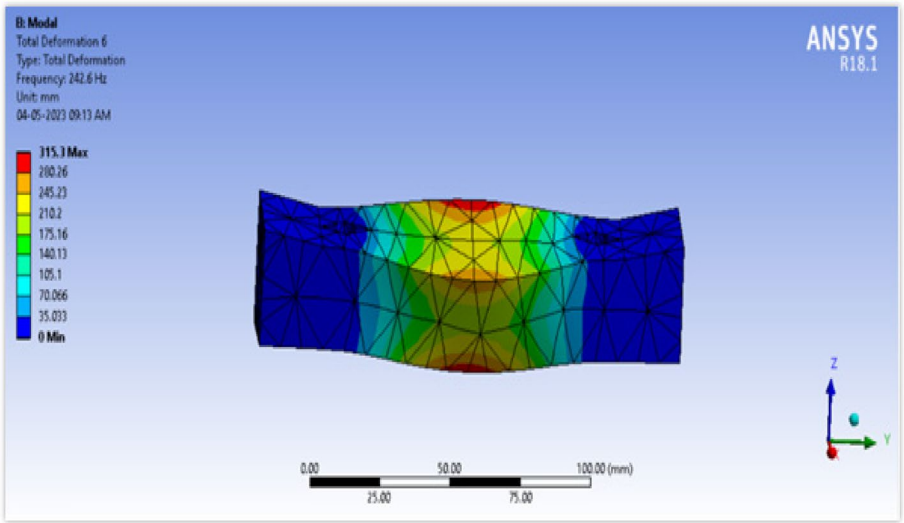

Fig. 41 Mode shape 5 for nitrile damper

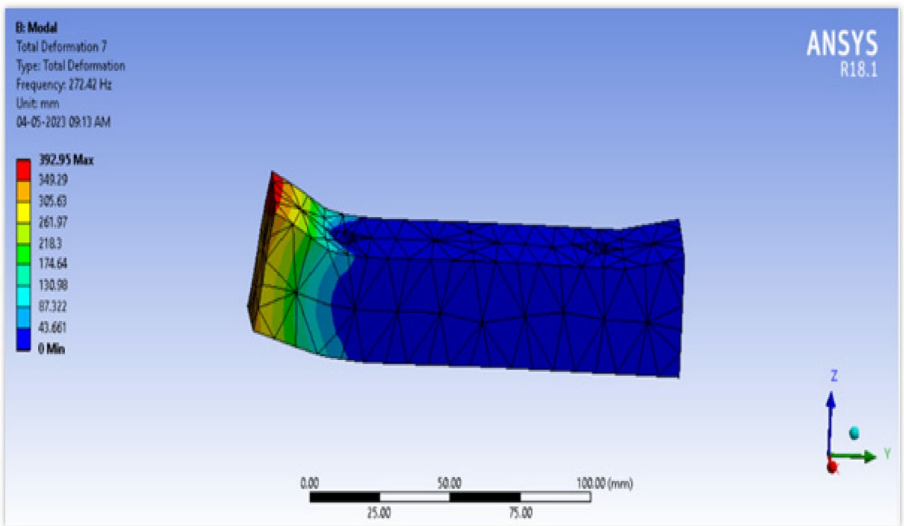

Fig. 42 Mode shape 6 for nitrile damper

Table 3 Modal analysis of concept design 3

Modal analysis of neoprene damper		Modal analysis of nitrile damper		Modal analysis of polyurethane damper	
Mode	**Frequency (Hz)**	**Mode**	**Frequency (Hz)**	**Mode**	**Frequency (Hz)**
1	92.107	1	131.02	1	153.71
2	115.64	2	164.71	2	192.97
3	126.69	3	180.46	3	211.43
4	133.45	4	190.09	4	222.71
5	145.37	5	207.06	5	242.6
6	163.24	6	232.52	6	272.42

Fig. 43 Design 1: neoprene material

Fig. 44 Design 1: nitrile material

Moreover, the probe's wide temperature ranging from -50 to +120 °C enables operation in extreme environmental conditions, ensuring adaptability and reliability across diverse operating environments.

In summary, the combination of the SKF Microlog Analyzer CMXA 75 and SKF Probe CMSS 2200 facilitates comprehensive and accurate vibration analysis, essential for condition monitoring and predictive maintenance in industrial settings. The robust design, precise measurements, and broad frequency range make this setup indispensable for diagnosing machinery health and optimizing operational efficiency.

Table 4 shows the FFT Specification used for taking the readings.

Fig. 45 Design 1: polyurethane material

Fig. 46 Design 2: neoprene material

View signal: By choosing spectrum in the view signal setting, a velocity vs. frequency graph was produced

Y-axis units: The magnitude of the vibrations was measured in velocity rms

Filter: Filer was set at 0.32 Hz so that undesirable frequencies below it would be removed

Frequency range: 500 Hz was selected as the frequency range

Fig. 47 Design 2: nitrile material

Fig. 48 Design 2: polyurethane material

Position selection of accelerometer probe

Real-time experimental values of transmitted and generated vibrations were obtained using an FFT analyzer. It was done using a 4 channel FFT analyzer. According to the diagram, the accelerometer probe for channel one was attached to the engine mount to measure vibrations that were generated, and the probe for channel two was attached to a chassis member to measure vibrations that were transmitted. These tremors are expressed in terms of rms velocity. Table 5 shows the FFT channel connections used.

Fig. 49 Design 3: neoprene material

Fig. 50 Design 3: nitrile material

Fig. 51 Design 3: polyurethane material

Fig. 52 SKF Microlog Analyzer

Experimental setup

In this setup shown in Fig. 54, Channel 1 (CH1) as shown in Fig. 55 is connected to the engine to capture the vibrations generated by its operation, while Channel 2 (CH2) as shown in Fig. 56 is connected to the chassis to measure the vibrations transmitted from the engine to the chassis. This arrangement allows for a comprehensive analysis of the vibrational behavior of the entire system, enabling engineers to understand how vibrations originating from the engine propagate and affect the chassis and surrounding components. Channel 1 provides insights into the vibrational characteristics directly generated by the engine during its operation. By monitoring CH1, engineers can assess the intensity, frequency, and pattern of vibrations produced by various engine components such as pistons, crankshafts, and camshafts. This information is crucial for diagnosing engine health, identifying potential issues such as misalignment or imbalance, and optimizing engine performance to reduce excessive vibrations. On the other hand, Channel 2 captures the vibrations experienced by the chassis due to the transmission of vibrations from the engine. These transmitted vibrations can impact vehicle performance, ride comfort, and overall durability.

Fig. 53 SKF Probe

Table 4 FFT specification

Number of channels	Ch1 and Ch2
Sensor	CMSS 2200
View signal	Spectrum and time
Y axis units	Velocity
Filter	0.32 Hz
Frequency range	500 Hz
Detection	RMS
Lines	1500

Table 5 FFT channel connections

Channel	Connections	Vibrations
Channel 1 (CH1)	Engine	To obtain generated vibrations
Channel 2 (CH2)	Chassis	To obtain transmitted vibrations

By monitoring CH2, engineers can evaluate the effectiveness of damping systems and isolation mechanisms designed to minimize the transmission of engine vibrations to the chassis. Additionally, CH2 data enables the identification of structural weak points in the chassis and the development of targeted solutions to enhance vibration attenuation and improve overall vehicle dynamics.

Results and discussion

Vibration analysis of existing design 1

Nitrile rubber damper

Figures 57, 58 and 59 show the reading of nitrile rubber damper at different rpm of existing design 1.

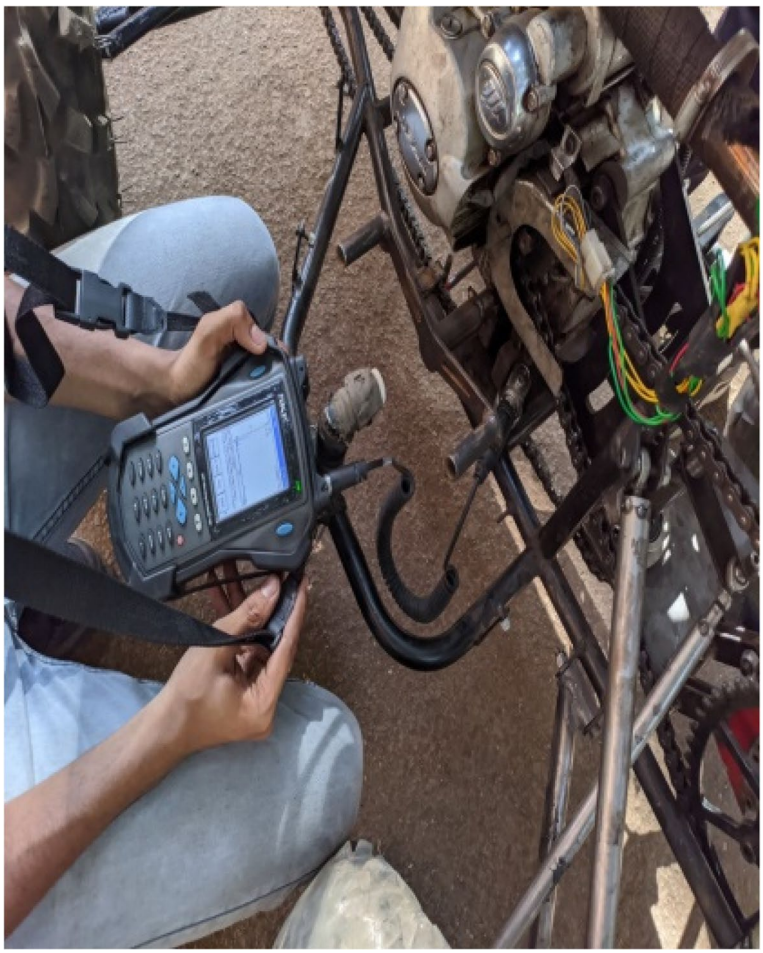

Fig. 54 Overall experimental setup on vehicle

Neoprene rubber damper

Figures 60, 61 and 62 show the reading of neoprene rubber damper at different rpm of existing design 1.

Polyurethane rubber damper

Figures 63, 64 and 65 show the reading of polyurethane rubber damper at different rpm of existing design 1.

Table 6 shows the result of different materials at different rpm for design 1.

The percentage reduction in vibration is calculated by comparing the vibration levels with and without the neoprene rubber dampers installed. Here's how it is calculated for each data point in the table:

For each data point:

- Subtract the vibration level without the damper (baseline) from the vibration level with the damper installed.
- Divide the result by the vibration level without the damper.

Fig. 55 Position of Channel 1

- Multiply the quotient by 100 to express the reduction as a percentage.

For example, let us calculate the percentage reduction for the first data point (20.8 for CH 1 at 2000–2500 RPM):

Percentage reduction = [(Vibration level without damper - Vibration level with damper) / Vibration level without damper] * 100

The percentage of vibration reduction in the provided table is determined through a systematic comparison of vibration levels across different RPM ranges for various materials. Firstly, measurements are taken at specific RPM intervals: 2000–2500, 4000–4500, and 6500–7000. For each RPM range, vibration levels are recorded for three distinct materials: nitrile, neoprene, and polyurethane. To calculate the percentage of vibration reduction for a given material at a particular RPM range, the difference between its vibration level and that of a reference material (presumably denoted as "CH 1" or "CH 2") is computed. This difference represents the reduction in vibration achieved by the specific material compared to the reference. Subsequently, this difference is divided by the vibration level of the reference material and multiplied by 100 to express it as a percentage. This calculation yields the percentage reduction in vibration attained by using the material in question compared to the

Fig. 56 Position of Channel 2

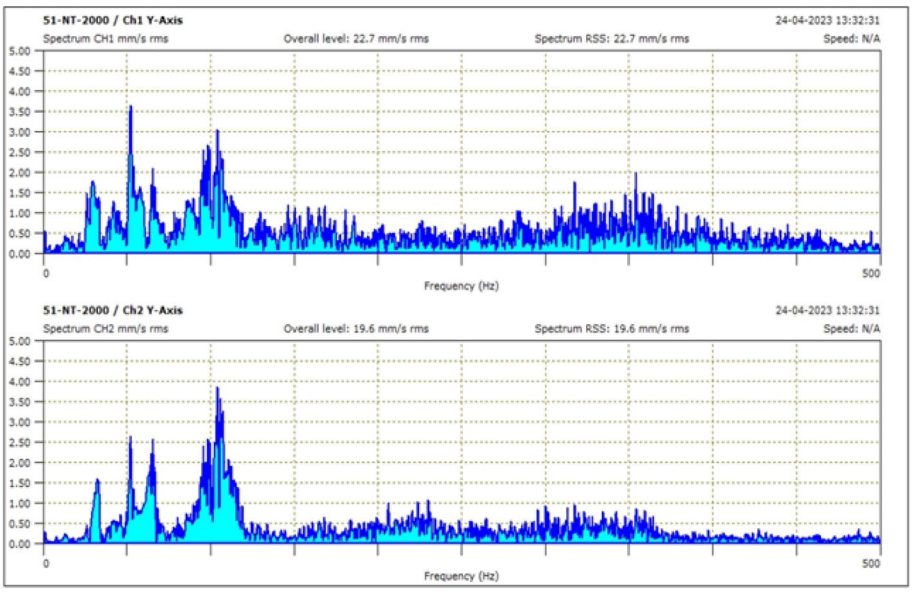

Fig. 57 Nitrile rubber damper at 2000–2500 Rpm

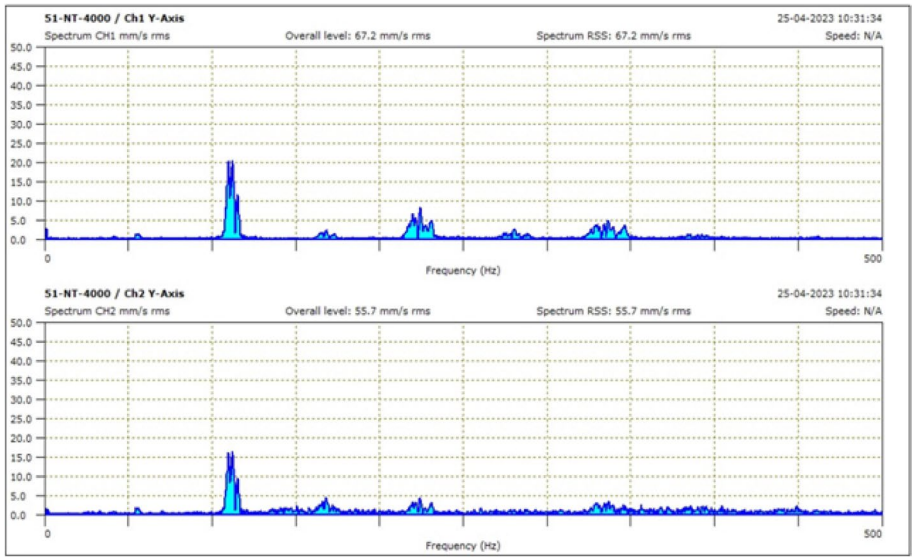

Fig. 58 Nitrile rubber damper at 4000–4500 Rpm

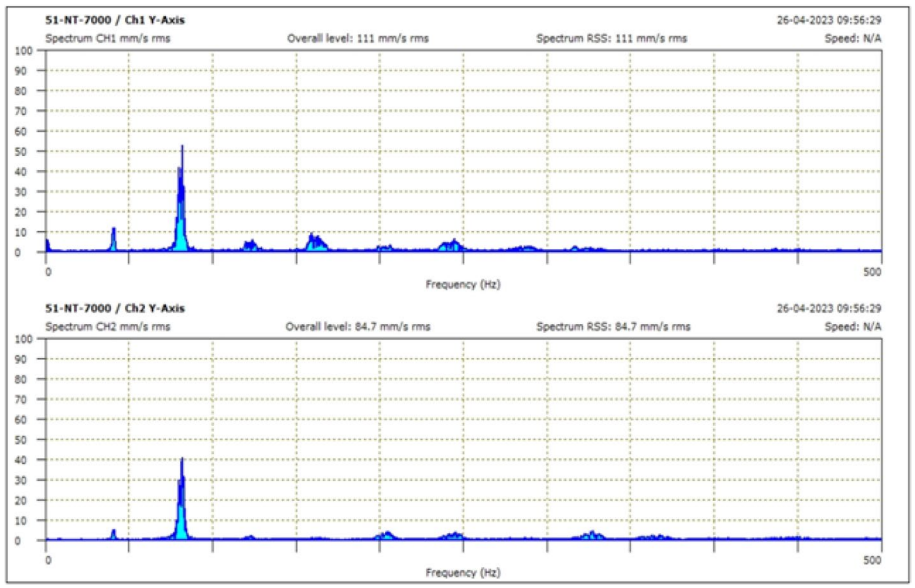

Fig. 59 Nitrile rubber damper at 6500–7000 Rpm

reference material. These calculated percentage reduction values are then presented in the table, allowing for a comparative analysis of the efficacy of different materials in reducing vibration across varied operating conditions and RPM ranges.

Vibration analysis on design 2

Nitrile rubber damper

Figures 66, 67 and 68 show the reading of nitrile rubber damper at different rpm of design 2.

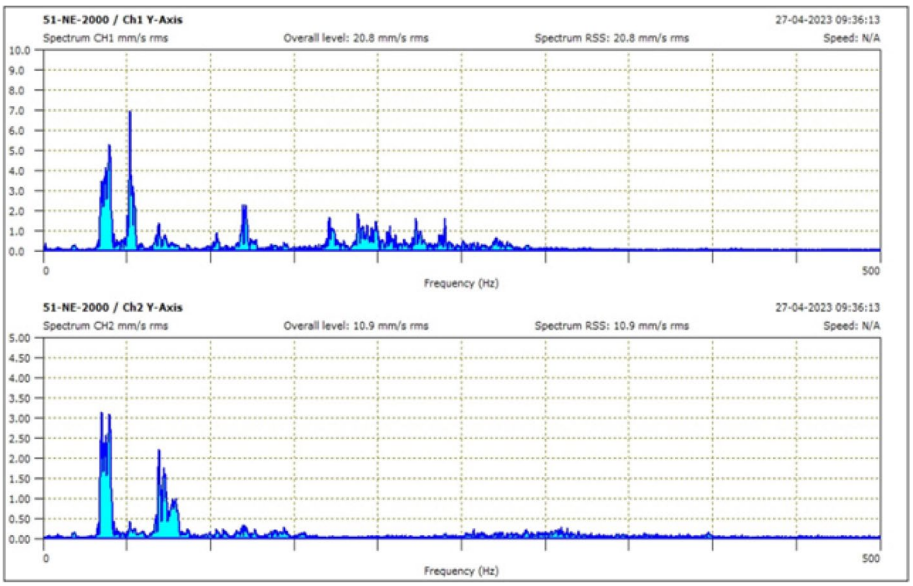

Fig. 60 Neoprene rubber damper at 2000–2500 Rpm

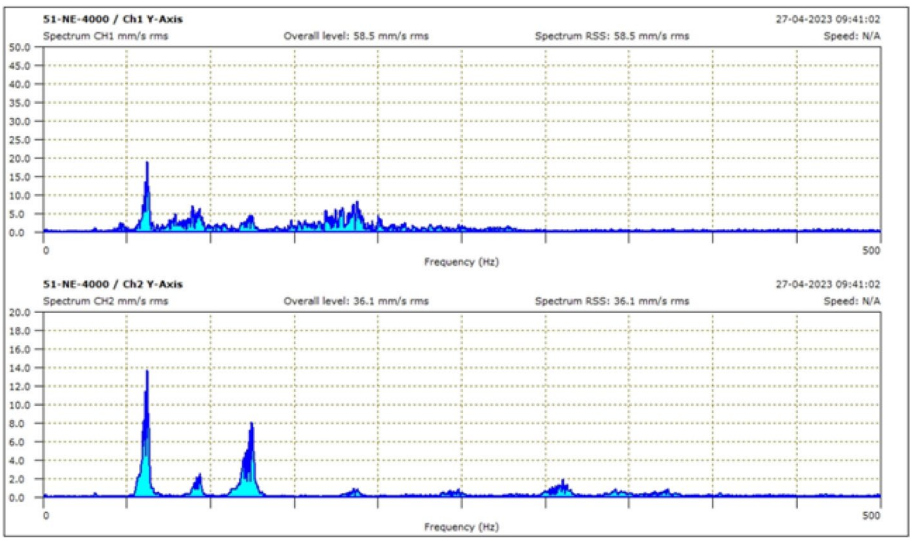

Fig. 61 Neoprene rubber damper at 4000–4500 Rpm

Neoprene rubber damper

Figures 69, 70 and 71 show the reading of neoprene rubber damper at different rpm of design 2.

Polyurethane rubber damper

Figures 72, 73 and 74 show the reading of neoprene rubber damper at different rpm of design 2.

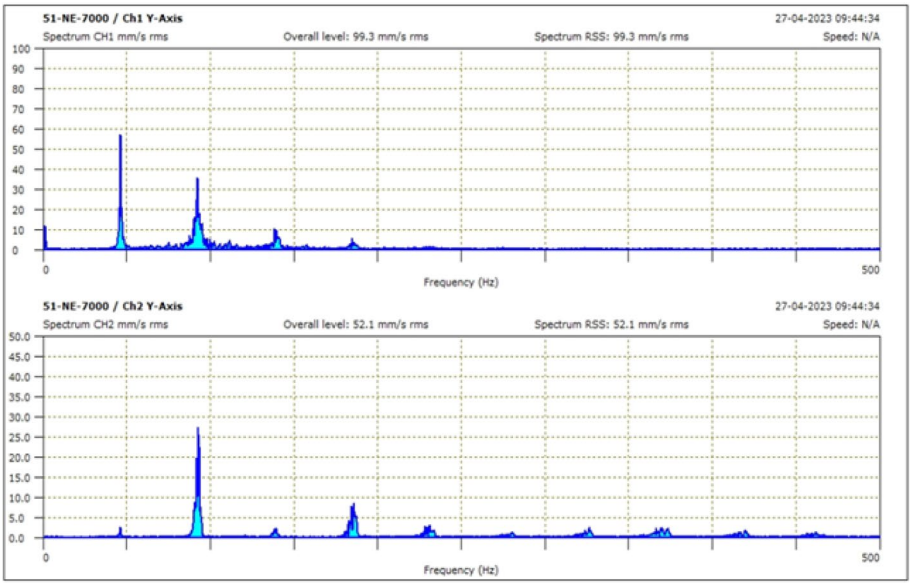

Fig. 62 Neoprene rubber damper at 6500–7000 Rpm

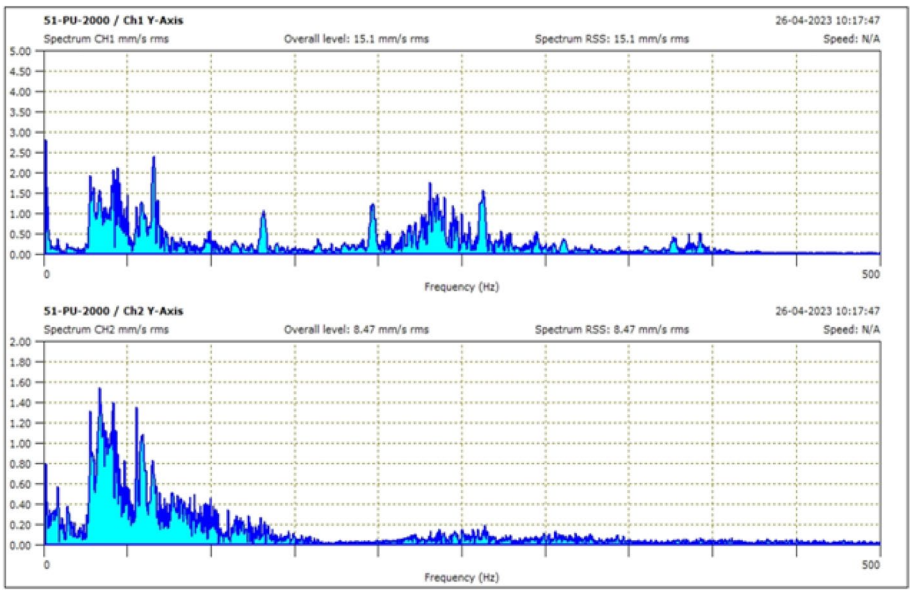

Fig. 63 Polyurethane rubber damper at 2000–2500 Rpm

Table 7 shows the result of different material at different rpm of design 2 and Fig. 76 shows the vibration reduction of each material for design 2.

Vibration analysis on design 3

Nitrile rubber damper

Figures 75, 76 and 77 show the reading of nitrile rubber damper at different rpm of design 3.

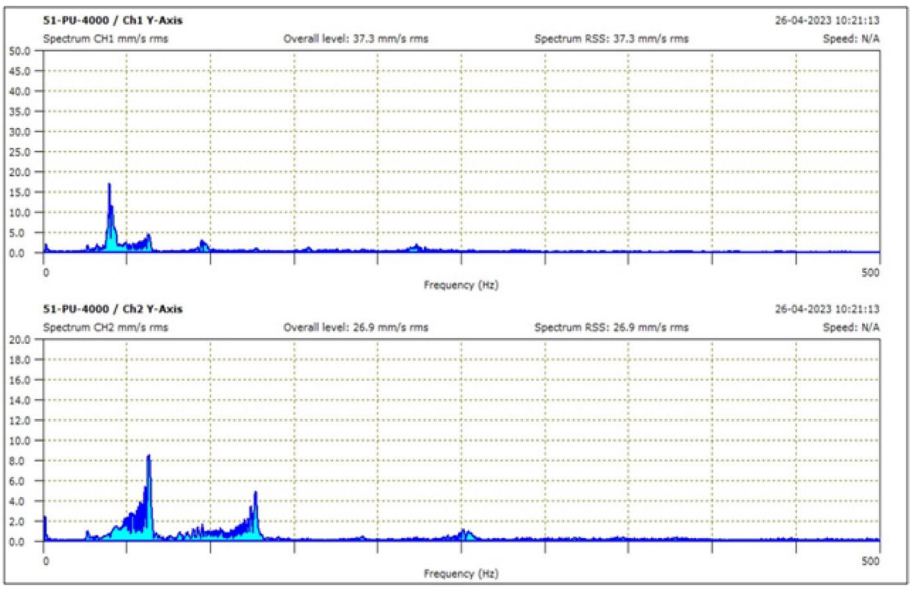

Fig. 64 Polyurethane rubber damper at 4000–4500

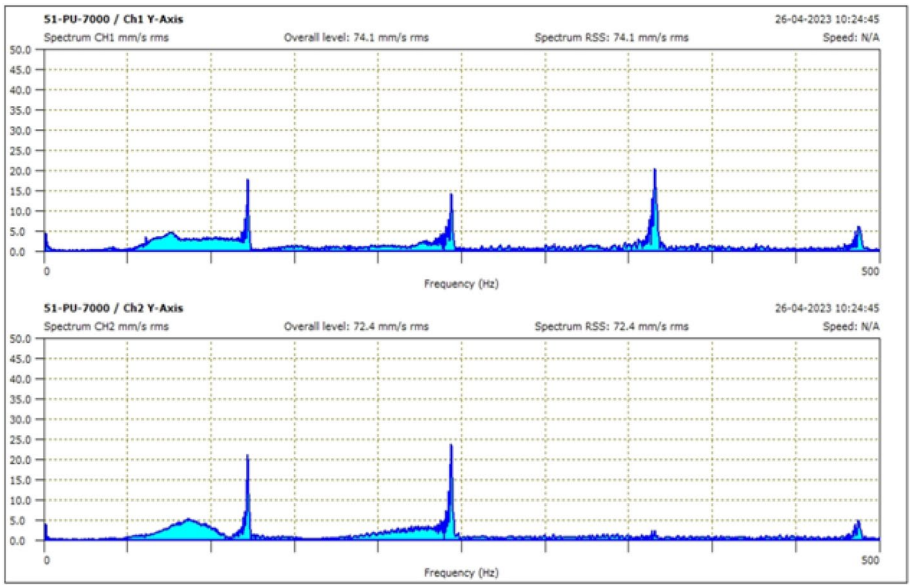

Fig. 65 Polyurethane rubber damper at 6500–7000 Rpm

Neoprene rubber damper

Figures 78, 79 and 80 show the reading of neoprene rubber damper at different rpm of design 3.

Table 6 Result table for design 1

Existing design 1									
Material	**RPM**								
	2000–2500			**4000–4500**			**6500–7000**		
	CH 1	**CH 2**	**% of vibration reduction**	**CH 1**	**CH 2**	**% of vibration reduction**	**CH 1**	**CH 2**	**% of vibration reduction**
Nitrile	22.7	18.7	17.62	39.2	36.7	6.38	111	84.7	23.69
Neoprene	20.8	10.9	47.6	58.5	36.1	38.29	99.3	52.1	47.53
Polyurethane	15.1	8.47	43.91	37.3	26.9	27.88	74	72	2.7

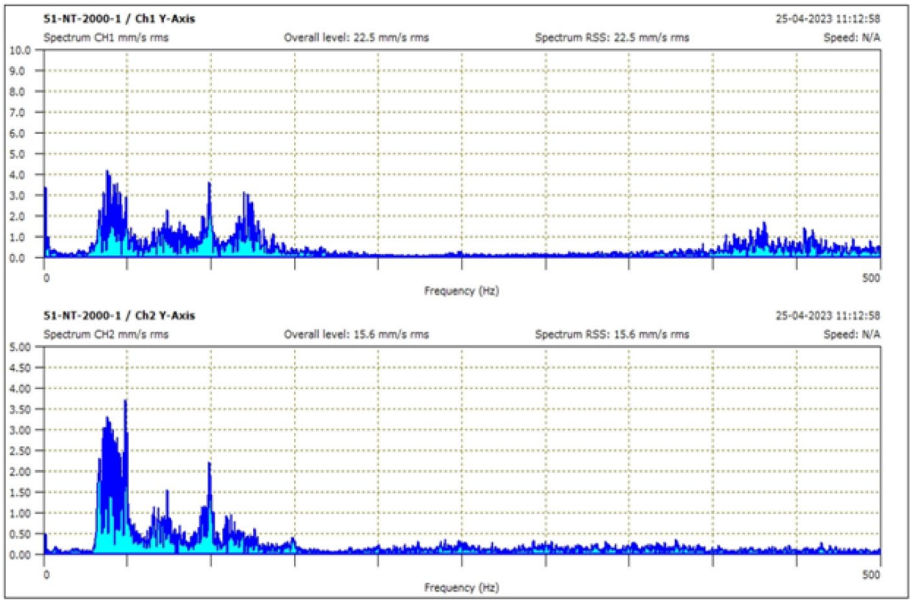

Fig. 66 Nitrile rubber damper at 2000–2500 Rpm

Polyurethane rubber damper

Figures 81, 82 and 83 show the reading of polyurethane rubber damper at different rpm of design 3.

Table 8 shows the result of different material at different rpm of design 3.

Table 9 shows the result of neoprene damper at different rpm of design 3.

The data presented in the table offers valuable insights into the efficacy of neoprene rubber dampers in attenuating engine vibrations across various RPM ranges and channels. Notably, the dampers consistently demonstrate significant vibration reduction percentages across all tested conditions. At lower RPM ranges (2000–2500), the dampers exhibit substantial effectiveness, achieving percentages ranging from 47.6% to 53.76%. Similarly, at mid-range (4000–4500) and higher RPM (6500–7000), the

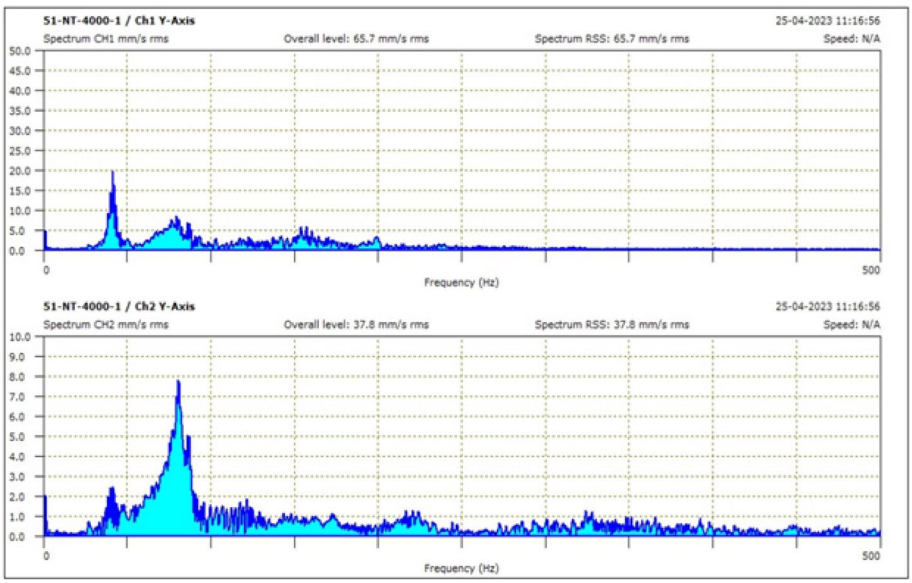

Fig. 67 Nitrile rubber damper at 4000–4500 Rpm

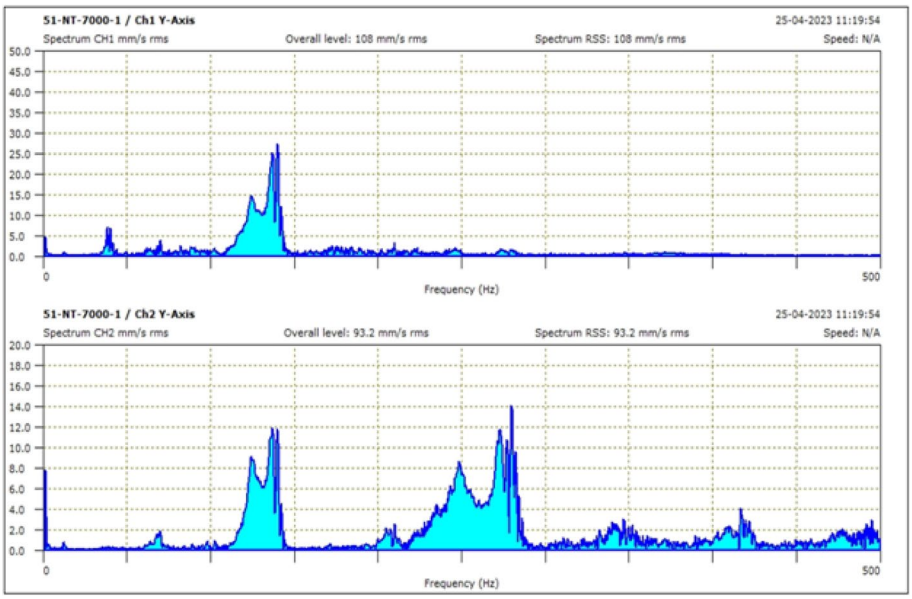

Fig. 68 Nitrile rubber damper at 6500–7000 Rpm

dampers maintain their effectiveness with percentages ranging from 36.1% to 53.85%. Although both channels (CH 1 and CH 2) generally show similar trends in vibration reduction, some instances of disparity between channels suggest potential variations in damping performance that warrant further investigation. Overall, the data

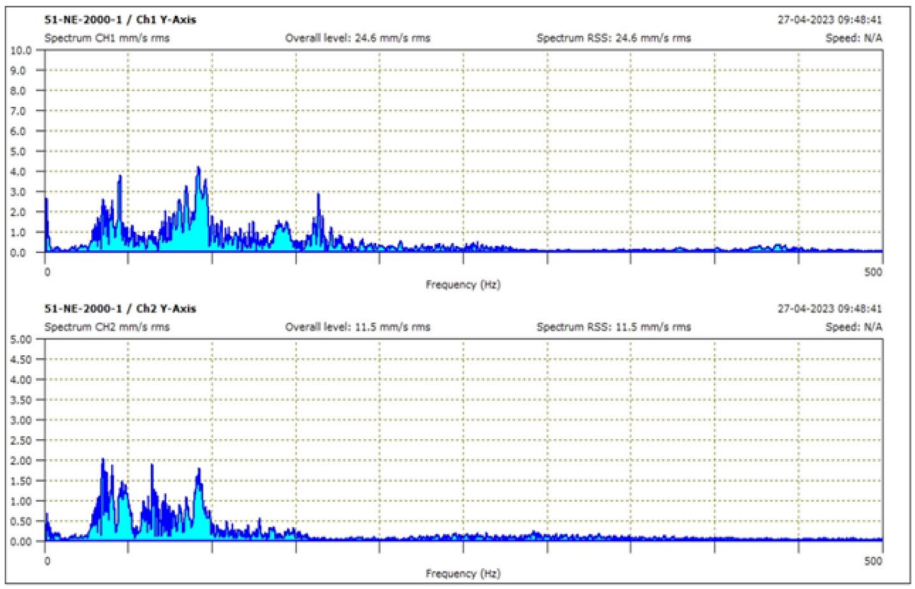

Fig. 69 Neoprene rubber damper at 2000–2500 Rpm

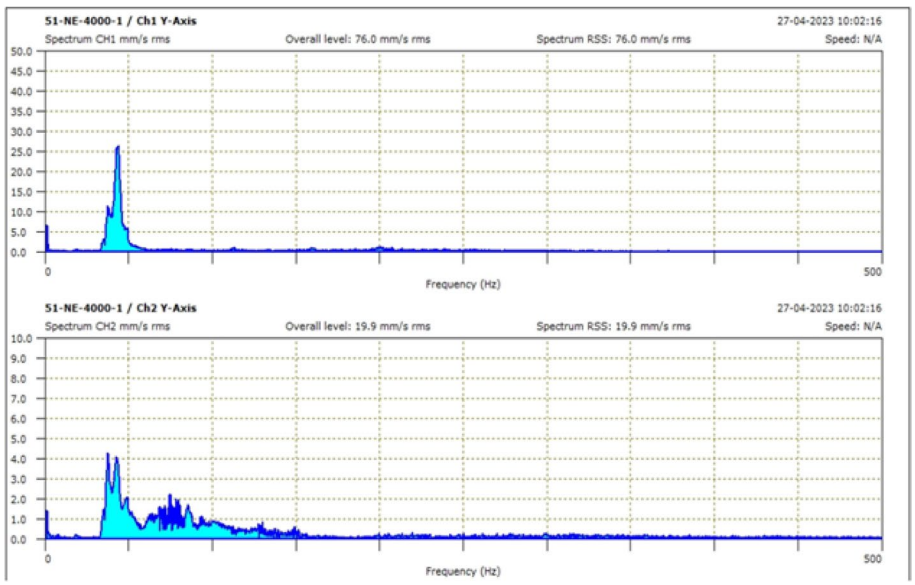

Fig. 70 Neoprene rubber damper at 4000–4500 Rpm

underscores the reliability and suitability of neoprene rubber dampers for mitigating engine vibrations in ATV quad bikes across diverse operating conditions. These findings not only affirm the effectiveness of neoprene rubber dampers but also suggest avenues for optimization and further research to enhance damping uniformity and overall performance.

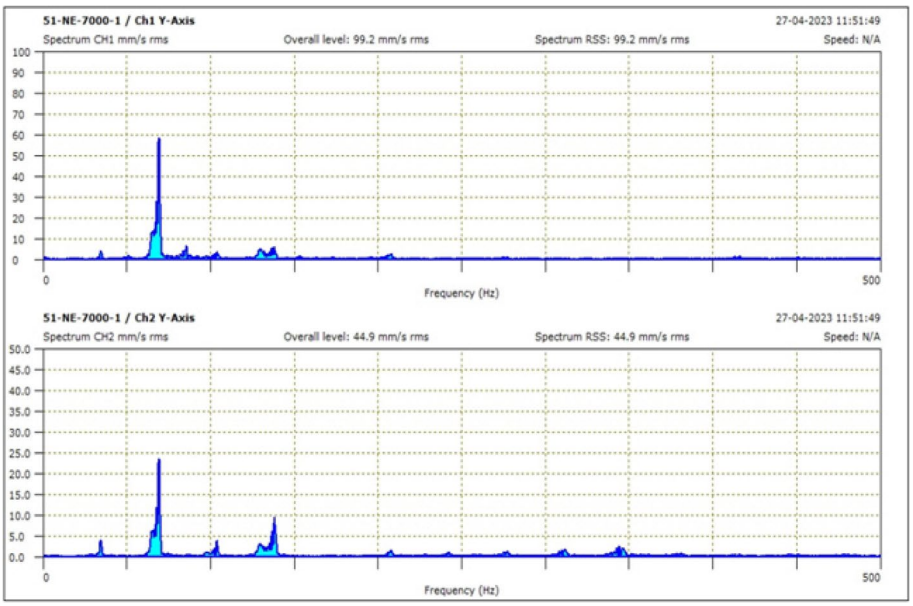

Fig. 71 Neoprene rubber damper at 6500–7000 Rpm

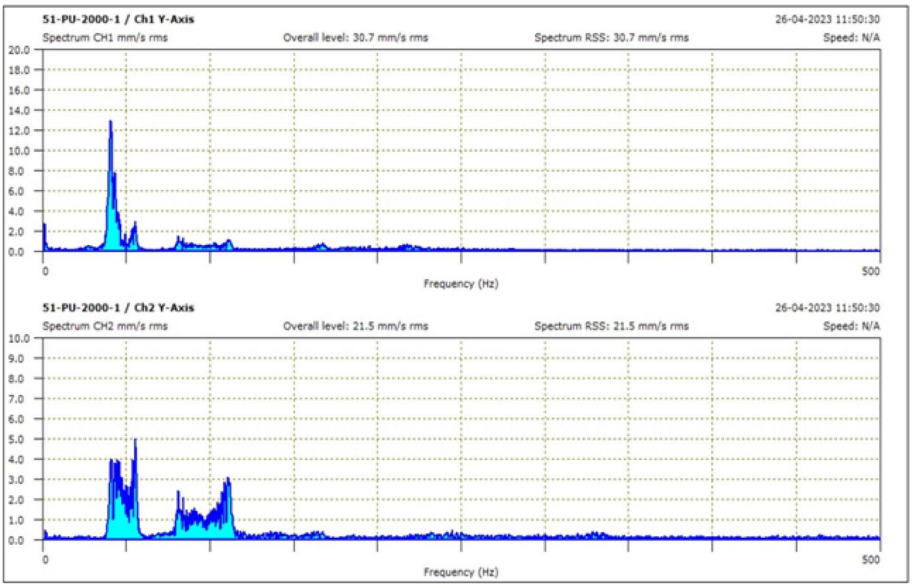

Fig. 72 Polyurethane rubber damper at 2000–2500 Rpm

Conclusions

Performed experiment and its analysis enlist remarkable points below:

1. Based on material properties, neoprene rubber is the best material for vibration dampers and has been empirically validated. (It is the best since it has a higher den-

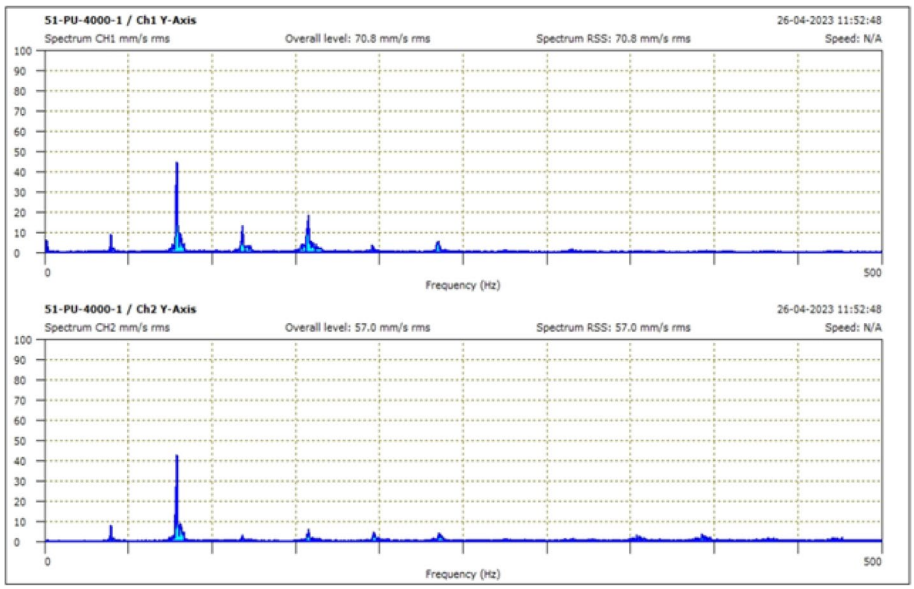

Fig. 73 Polyurethane rubber damper at 4000–4500 Rpm

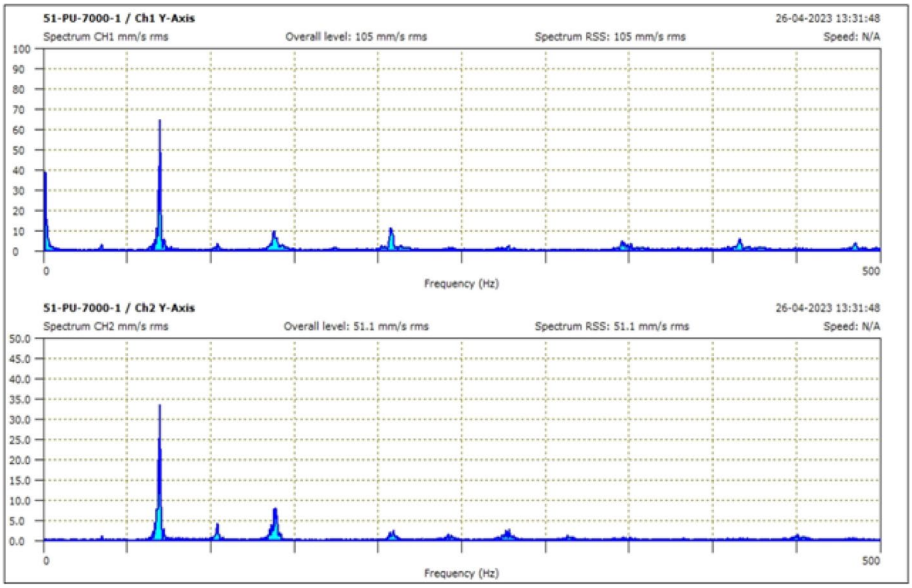

Fig. 74 Polyurethane rubber damper at 6500–7000 Rpm

sity than the other materials considered.) Neoprene rubber is well recognized, along with its resistance to corrosion, heat, and grease. Furthermore, although density is one component that may influence a vibration damper's performance, it is not always

Table 7 Result table design 2

Material	RPM								
	2000–2500			4000–4500			6500–7000		
	CH 1	CH 2	% of vibration reduction	CH 1	CH 2	% of vibration reduction	CH 1	CH 2	% of vibration reduction
Nitrile	22.5	17.5	22.22	65.7	37.8	42.47	108	93.7	13.24
Neoprene	24.6	11.5	53.25	76.6	18.9	75.33	99	44	55.56
Polyurethane	30.7	21.7	29.32	70.8	57.6	18.64	105	51	51.43

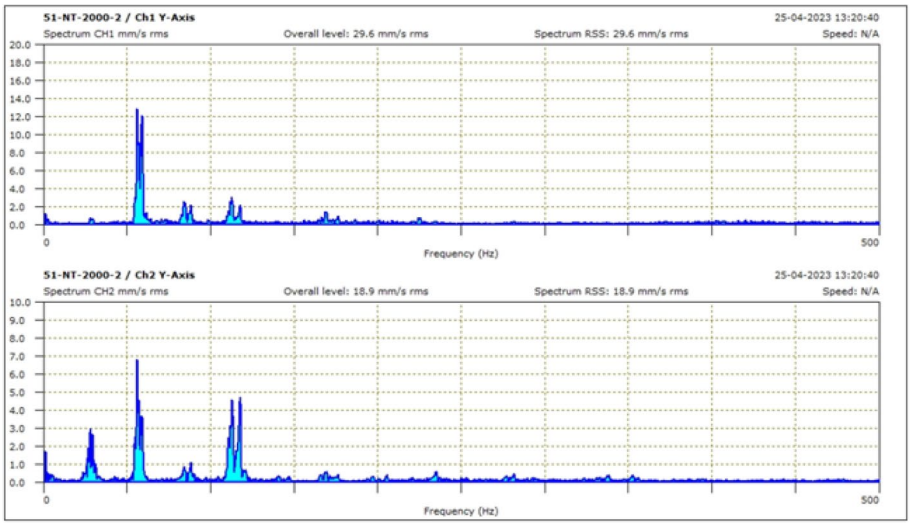

Fig. 75 Nitrile rubber damper at 2000–2500 Rpm

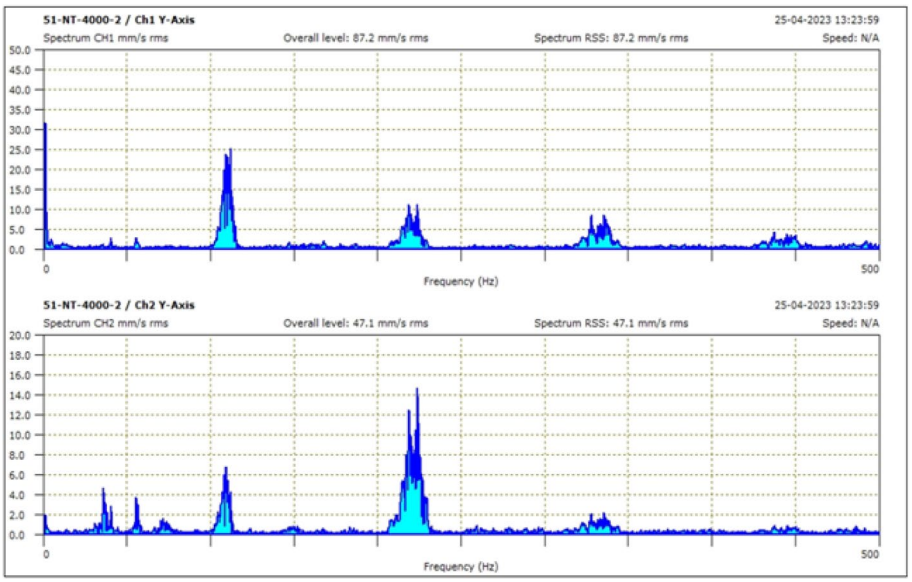

Fig. 76 Nitrile rubber damper at 4000–4500 Rpm

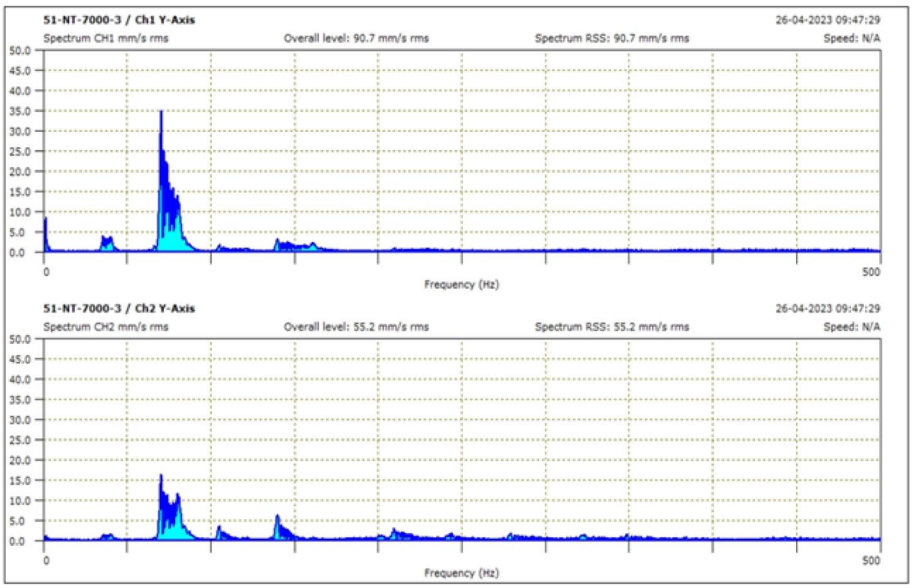

Fig. 77 Nitrile rubber damper at 6500–7000 Rpm

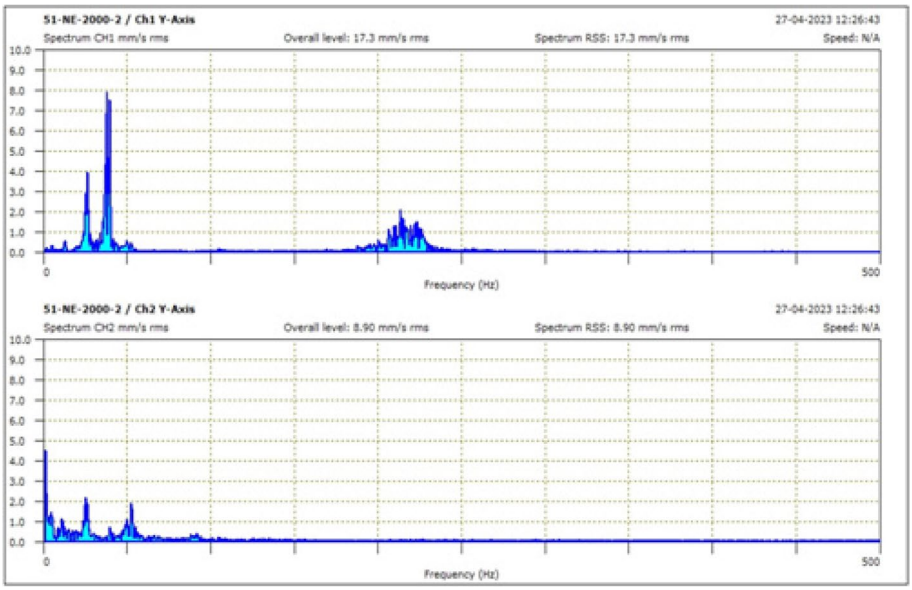

Fig. 78 Neoprene rubber damper at 2000–2500 Rpm

the sole or most significant factor. In addition to elasticity, stiffness, and damping coefficient, other material characteristics can also have a big impact on how effective a vibration damper is.

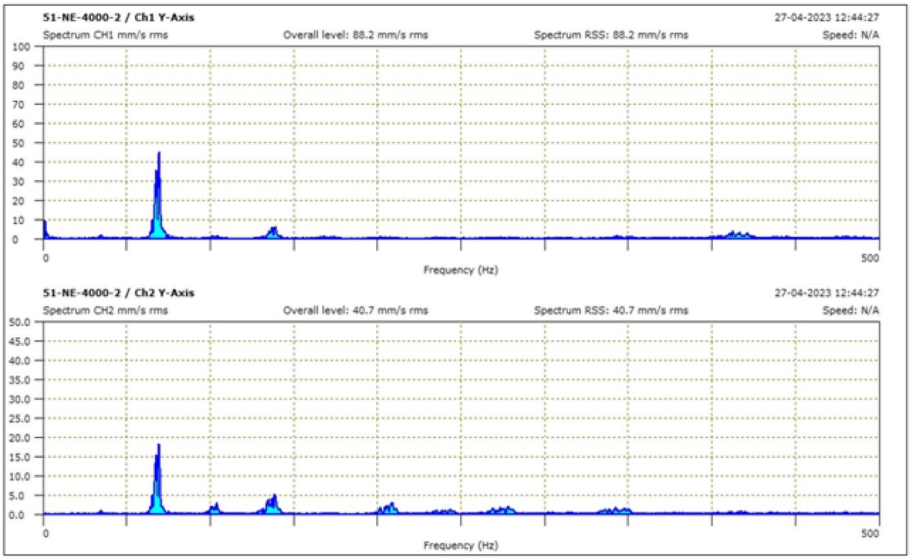

Fig. 79 Neoprene rubber damper at 4000–4500 Rpm

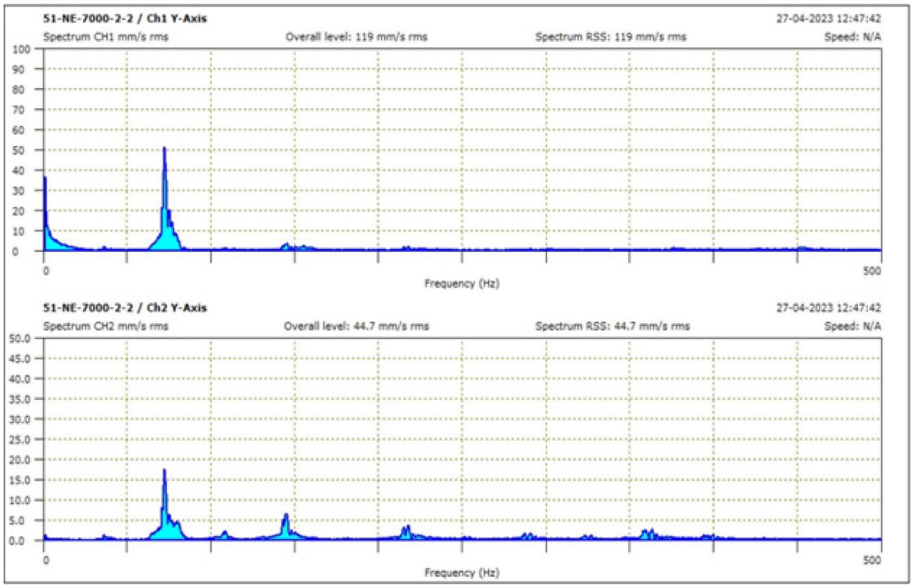

Fig. 80 Neoprene rubber damper at 6500–7000 Rpm

2. Design 3 of the vibration dampers reduces vibration by up to 62% more than Design 2, which is second best and reduces vibration by 55.56%, and Design 1, which reduces vibration by 47.53%. The efficiency of a vibration damper can, however, is affected by a number of variables, including the particular application, the frequency and ampli-

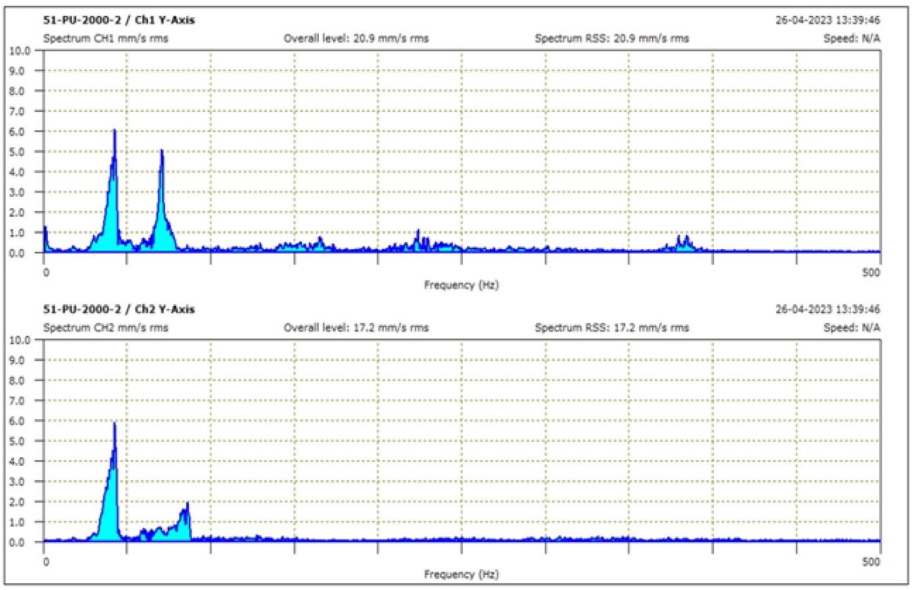

Fig. 81 Polyurethane rubber damper at 2000–2500 Rpm

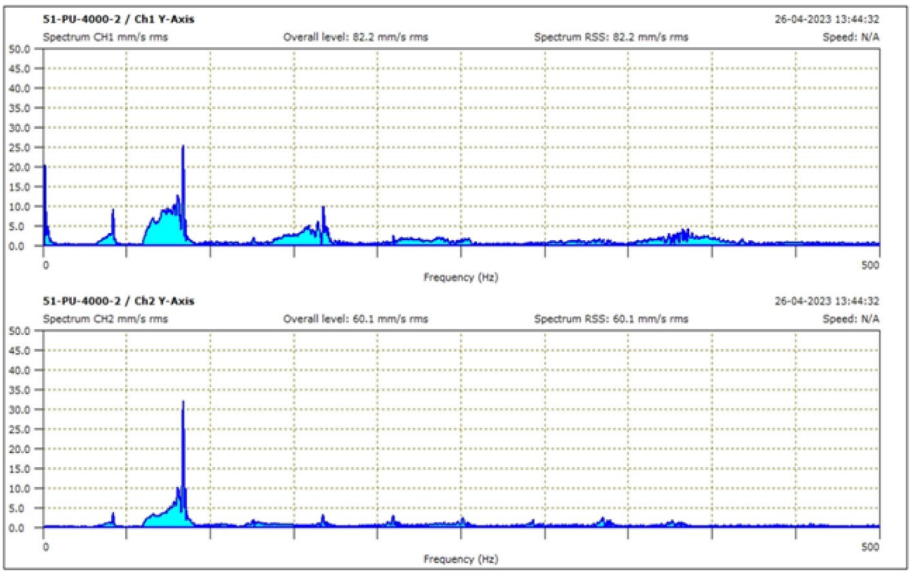

Fig. 82 Polyurethane rubber damper at 4000–4500 Rpm

tude of the vibration, as well as the weight and size of the machinery. Therefore, even though these findings imply that Design 3 might be the most effective option given the application and conditions, it might not always be the best option for every type of engine and situations.

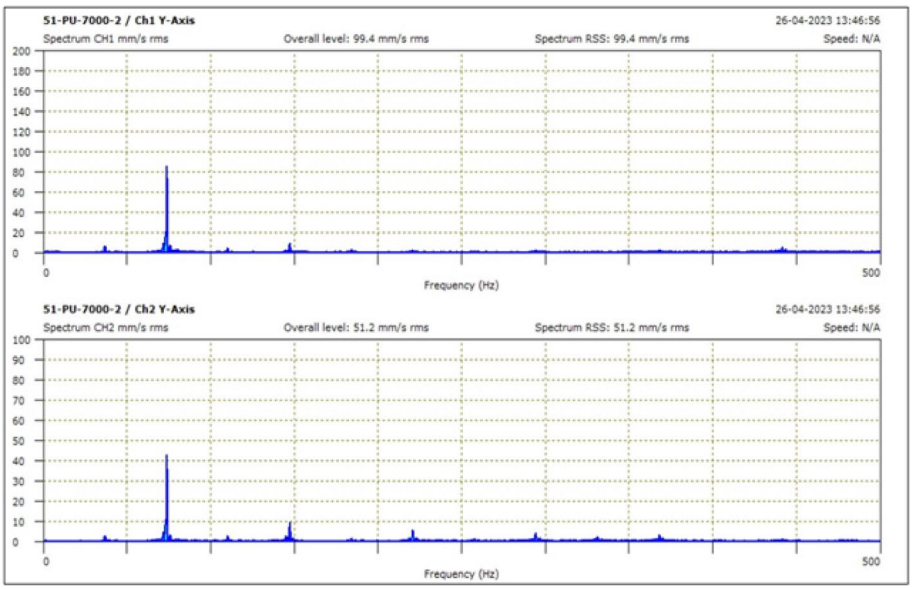

Fig. 83 Polyurethane rubber damper at 6500–7000 Rpm

Table 8 Result table design 3

Material	RPM								
	2000–2500			4000–4500			6500–7000		
	Ch 1	Ch 2	% of vibration reduction	Ch 1	Ch 2	% of vibration reduction	Ch 1	Ch 2	% of vibration reduction
Nitrile	29.6	18.9	36.15	87.2	47.2	45.87	90.7	55.2	39.14
Neoprene	17.3	8	53.76	88.2	40.7	53.85	119	44.7	62.44
Polyurethane	20.9	17.2	17.7	82.2	60.1	26.89	99.4	51.2	48.49

Table 9 Result table for neoprene damper

Neoprene rubber									
Design	RPM								
	2000–2500			4000–4500			6500–7000		
	Ch 1	Ch 2	% of vibration reduction	Ch 1	Ch 2	% of vibration reduction	Ch 1	Ch 2	% of vibration reduction
1	20.8	10.9	47.6	58.5	36.1	38.29	99.3	52.1	47.53
2	24.6	11.5	53.25	76.6	18.9	75.33	99	44	55.56
3	17.3	8	53.76	88.2	40.7	53.85	119	44.7	62.44

3. Neoprene, nitrile, and polyurethane are the three composite materials. According to measurements from an FFT analyzer, which may reduce vibration by up to 62% compared to more other materials, neoprene stands out as the best material.

Abbreviations

NVH	Noise vibration harshness
ATV	All-terrain vehicle
FFT	Fast Fourier transform
APDL	ANSYS parametric design language
.catpart	Part model file extension in CATIA
ALTAIR	software for innovative design and engineering
C	Damping factor

Acknowledgements
Not applicable.

Authors' contributions
PB: conceptualization, methodology, investigation, resources, writing-original and revised draft, supervision and project administration. NV: investigation, visualization and writing-original and revised draft. All authors have read and approved the manuscript.

Funding
There is no funding.

Availability of data and materials
The datasets/readings will be shared upon request.

Declarations

Research involving human participants and/or animals
There is no involvement with human participants and/or animals.

Competing interests
The authors declare no competing interests.

Received: 25 March 2024 Accepted: 4 June 2024
Published online: 14 June 2024

References

1. L. Clay, G. J. Treharne, E. J. C. Hay-Smith, and S. Milosavljevic, 'Are agricultural quad bike loss-of-control events driven by unrealistic optimism?', *Saf. Sci.*, vol. 66, 2014, https://doi.org/10.1016/j.ssci.2014.02.002
2. Y. Wang, P. Pan, K. Deng, T. Takada, and F. He, 'Experimental study on high-damping viscoelastic rubber coupling beam damper', *Jianzhu Jiegou XuebaoJournal Build. Struct.*, vol. 38, no. 3, 2017, https://doi.org/10.14006/j.jzjgxb.2017.03.018
3. R. C. Franklin, K. E. McBain-Rigg, and S. M. Knight, 'Factors to be considered in developing occupational regulations for quad bikes in Australia', *J. Agromedicine*, vol. 20, no. 3, 2015, https://doi.org/10.1080/1059924X.2015.1047108
4. Y. Tu, G. Yang, Q. Cai, L. Wang, and H. Yin, 'Dynamical analysis and experimental verification of deviation angles caused by rubber dampers deformation in high precision mechanically dithered RLG dual-axis RINS', *Mech. Syst. Signal Process.*, vol. 126, 2019, https://doi.org/10.1016/j.ymssp.2019.02.045
5. Z. D. Xu, Y. Yang, Y. N. Zhu, and T. Ge, 'Experimental study and mathematical modeling of viscoelastic dampers with wider temperature range based on blended rubber matrix', *J. Build. Eng.*, vol. 70, 2023, https://doi.org/10.1016/j.jobe.2023.106414
6. S. Fujita *et al.*, 'Vibration control of high-rise buildings using high-damping rubber damper (2nd Report, Loading Tests and Design Formula for Cylinder-Type High-Damping Rubber Damper)', *Trans. Jpn. Soc. Mech. Eng. Ser. C*, vol. 61, no. 585, 1995, https://doi.org/10.1299/kikaic.61.1885
7. R. C. Franklin, S. Knight, and T. Lower, 'Mount Isa statement on quad bike safety', *Rural Remote Health*, vol. 14, no. 3, 2014, https://doi.org/10.22605/rrh2687
8. R. Suntako, 'The rubber damper reinforced by modified silica fume (mSF) as an alternative reinforcing filler in rubber industry', *J. Polym. Res.*, vol. 24, no. 8, 2017, https://doi.org/10.1007/s10965-017-1293-5
9. P. Lundqvist, C. Stave, and E. Göransson, 'Parents' risk acceptance and attitudes toward the use of quad bikes by children and young people in Sweden', *J. Agric. Saf. Health*, vol. 28, no. 1, 2022, https://doi.org/10.13031/jash.14558
10. K. A. Vuong, I. Lewis, K. Vallmuur, and A. Watson, 'Identifying foci for safety messages targeting child injury from driving quad bikes: a critical beliefs analysis of parental beliefs in Australia', *J. Safety Res.*, vol. 85, 2023, https://doi.org/10.1016/j.jsr.2023.04.010
11. S. Milosavljevic *et al.*, 'Factors associated with quad bike loss of control events in agriculture', *Int. J. Ind. Ergon.*, vol. 41, no. 3, 2011, https://doi.org/10.1016/j.ergon.2011.02.010
12. J. J. Sonia, P. Jayachandran, A. Q. Md, S. Mohan, A. K. Sivaraman, and K. F. Tee, 'Machine-learning-based diabetes mellitus risk prediction using multi-layer neural network no-prop algorithm', *Diagnostics*, vol. 13, no. 4, 2023, https://doi.org/10.3390/diagnostics13040723
13. S. E. Liddle, K. M. McDermott, L. M. Ward, H. H. Lim, and D. J. Read, 'Quad bike injuries at an Australian regional hospital: a trauma registry review', *ANZ J. Surg.*, vol. 90, no. 4, 2020, https://doi.org/10.1111/ans.15631
14. C. Rajkumar, S. Jayavelu, and R. R. Kumar, 'Design and analysis of damper spring and its structural components', *Int. J. Civ. Eng. Technol.*, vol. 8, no. 10, 2017

15. Y. Zhou, D. Li, F. Shi, W. Luo, and X. Deng, 'Experimental study on mechanical properties of the hybrid lead viscoelastic damper', *Eng. Struct.*, vol. 246, 2021, https://doi.org/10.1016/j.engstruct.2021.113073
16. H. Qian, D. Wei, Y. Shi, Z. Li, and H. Li, 'Pre-tensioned SMA cable tests and its application in a novel self-centering viscoelastic damper', *Soil Dyn. Earthq. Eng.*, vol. 168, 2023, https://doi.org/10.1016/j.soildyn.2023.107850
17. Y. Nurchasanah, B. Suhendro, and I. Satyarno, 'Properties and design of engine mounting rubber automotive as damper for building retrofitting', *Int. J. GEOMATE*, vol. 25, no. 108, 2023, https://doi.org/10.21660/2023.108.3725
18. Prasetya HW, Atmaja DS, Pamungkas HD (2021) RANCANG BANGUN RUBBER DAMPER PADA LORI INSPEKSI ELEKTRIK. JNANALOKA. https://doi.org/10.36802/jnanaloka.2021.v2-no1-27-34
19. G. Maddaloni, N. Caterino, and A. Occhiuzzi, 'Shake table investigation of a structure isolated by recycled rubber devices and magnetorheological dampers', *Struct. Control Health Monit.*, vol. 24, no. 5, 2017, https://doi.org/10.1002/stc.1906
20. Y. Xu, X. Cheng, W. Ke, Q. X. Zhu, Y. L. He, and Y. Zhang, 'SMOTE-based fault diagnosis method for unbalanced samples', in *Proceedings of 2022 IEEE 11th Data Driven Control and Learning Systems Conference, DDCLS 2022*, 2022. https://doi.org/10.1109/DDCLS55054.2022.9858365
21. A. Modhej and S. M. Zahrai, 'Experimental study of high axial damping rubber (HADR) in new viscoelastic dampers', *J. Test. Eval.*, vol. 48, no. 6, 2020, https://doi.org/10.1520/JTE20180104
22. S. K. Busse, A. N. Sinclair, D. T. Redda, and D. H. Wondimu, 'Evaluation of the vibration characteristics and handle vibration damping of diesel-fueled 15-HP single-axle tractor', *Adv. Mech. Eng.*, vol. 13, no. 8, 2021, https://doi.org/10.1177/16878140211040648
23. P. S. Badkar and M. M. Benal, 'Estimation of damping ratio of silicone rubber using half power bandwidth method', *Mater. Today Proc.*, vol. 59, 2022, https://doi.org/10.1016/j.matpr.2021.12.219
24. S. J. E. Becker, A. G. J. Bot, S. E. Curley, J. B. Jupiter, and D. Ring, 'A prospective randomized comparison of neoprene vs thermoplast hand-based thumb spica splinting for trapeziometacarpal arthrosis', *Osteoarthritis Cartilage*, vol. 21, no. 5, 2013, https://doi.org/10.1016/j.joca.2013.02.006
25. A. Das and P. Mahanwar, 'A brief discussion on advances in polyurethane applications', *Advanced Industrial and Engineering Polymer Research*, vol. 3, no. 3. 2020. https://doi.org/10.1016/j.aiepr.2020.07.002
26. R. Egelkamp, T. Zimmermann, D. Schneider, R. Hertel, and R. Daniel, 'Impact of nitriles on bacterial communities', *Front. Environ. Sci.*, vol. 7, no. JUL, 2019, https://doi.org/10.3389/fenvs.2019.00103
27. J. Gibbs, C. Sheridan, F. Khorsandi, and A. M. Yoder, 'Perspective: emphasizing safe engineering design features of quad bikes in agricultural safety programs', *J. Agric. Saf. Health*, vol. 29, no. 2, 2023, https://doi.org/10.13031/jash.15351
28. L. Toma, E. Bompard, and A. Mazza, 'Modal analysis', in *converter-based dynamics and control of modern power systems*, 2020. https://doi.org/10.1016/B978-0-12-818491-2.00004-3
29. P. Frankovský, I. Delyová, P. Sivák, J. Bocko, J. Živčák, and M. Kicko, 'Modal analysis using digital image correlation technique', *Materials*, vol. 15, no. 16, 2022, https://doi.org/10.3390/ma15165658
30. K. Worden and P. L. Green, 'A machine learning approach to nonlinear modal analysis', *Mech. Syst. Signal Process.*, vol. 84, 2017, https://doi.org/10.1016/j.ymssp.2016.04.029